https://doi.org/10.5194/egusphere-2026-2571
Preprint. Discussion started: 21 May 2026

Seasonal and spatio-temporal dynamics of marine heatwaves in the Senegalo–Mauritanian Upwelling System and chlorophyll-a responses

Waly Dione[1], Ibrahima Camara[1,3], Alban Lazar[2], Diana Ruiz-Pino[2], and Amadou Thierno Gaye[1]

[1]Laboratoire Physique de l'Atmosphère et de l'Océan-Siméon Fongang (LPAO-SF), Ecole Supérieure Polytechnique (ESP), Université Cheikh Anta Diop de Dakar, Dakar-Fann 5085, Dakar, Senegal
[2]LOCEAN, Université Pierre & Marie Curie, Courrier 134, 4 pl. Jussieu, 75252 Paris Cedex 05, France
[3]Université Amadou Mahtar Mbow (UAM), Rue 21x20, 2ème Arrondissement, Pôle Urbain de Diamniadio - BP : 45927 Dakar, SÉNÉGAL

Correspondence: Waly DIONE (waly1.dione@ucad.edu.sn)

Abstract. Marine heatwaves (MHWs) represent an increasing threat to marine ecosystems, yet their dynamics remain poorly documented in tropical eastern boundary upwelling systems, where upwelling reaches its maximum in boreal winter rather than in summer. This study analyses the spatio-temporal variability of MHWs, their physical drivers, and biological impacts in the Senegalo-Mauritanian Upwelling System (SMUS) over 1982–2024, using satellite-derived SST, chlorophyll-a, and atmospheric reanalysis data.

A strong spatial heterogeneity is observed, with the highest cumulative number of MHW days (up to 50 days per year) occurring in shallow regions weakly influenced by upwelling, as well as in offshore transition zones. In contrast, lower occurrences (around 25 days per year) are observed in persistent upwelling areas, particularly at Cap Blanc and along the Petite Côte, which act as relative thermal refuges. At the seasonal scale, MHWs are more frequent and more persistent during the CP, particularly south of 18°N, while their intensity is modulated by the seasonal migration of the upwelling front. Over the 42-year period, the Grande Côte region emerges as the most vulnerable coastal zone, showing the strongest increase in MHW occurrence, with significant trends ($p<0.05$) in total MHW days (+10.25 days decade^{-1}) and duration (+2.22 days decade^{-1}). Along the Petite Côte, trends are approximately four times stronger during the CP (+5.16 days decade^{-1}) than during the warming period (+1.34 days decade^{-1}). No significant long-term trend is detected for maximum intensity at the annual scale. However, a significant seasonal increase (+0.16 °C per decade) is identified during the warming period in the Grande Côte region. Cap Blanc shows remarkable stability across all indicators, highlighting the buffering capacity of permanent upwelling.

Composite analysis of 283 MHW events identifies wind relaxation as the primary driver, reducing Ekman pumping and weakening upwelling circulation. However, the oceanic response differs strongly between regions. In the northern SMUS (Cap Blanc), where upwelling is quasi-permanent, MHWs are moderate and adjust rapidly, reflecting a thermodynamically dominated regime. In contrast, in southern regions with seasonal upwelling, wind relaxation leads to a near-complete collapse of upwelling, resulting in stronger and more persistent heat accumulation, characteristic of a dynamically controlled regime. These physical contrasts translate into distinct biological responses. In the southern SMUS, MHWs lead to a systematic decrease in chlorophyll-a (up to -2 mg m^{-3}). In contrast, Cap Blanc exhibits a season-dependent response, with an increase

https://doi.org/10.5194/egusphere-2026-2571
Preprint. Discussion started: 21 May 2026

in biomass (up to +3 mg m^{-3}) during the CP, sustained by residual nutrient supply and moderate warming, and a decrease in biomass (up to -2.7 mg m^{-3}) during the warming period due to enhanced stratification. These results highlight the crucial role of local upwelling dynamics in modulating the characteristics of MHWs and their ecological impacts in this marine ecosystem of major socio-economic importance.

Keywords: Marine heatwaves; chlorophyll-a, Senegal–Mauritania Upwelling System; Canary Current System; seasonal variability.

1 Introduction

Marine heatwaves represent one of the most abrupt manifestations of anthropogenic ocean warming, with their frequency nearly doubling since the 1980s (Oliver et al., 2018) and causing major impacts on biodiversity and food security (Smale et al., 2019). In eastern boundary upwelling systems (EBUS), which concentrate 20% of the global marine biomass on just 1% of the ocean surface (Pauly and Christensen, 1995; Messié and Chavez, 2015), the dynamics of MHWs are particularly complex. Upwelling, by bringing cold and nutrient-rich waters to the surface, acts as a thermal buffer that locally moderates the occurrence of extreme events (Varela et al., 2021; DeCastro et al., 2014; Seabra et al., 2019). However, this resilience is neither uniform nor permanent, as it is influenced by the intensity and seasonality of Ekman pumping processes (García-Reyes et al., 2023; Seabra et al., 2019) and their interaction with large-scale atmospheric forcings (Holbrook et al., 2019; Schlegel et al., 2021). Furthermore, Wang et al. (2023) showed that this buffering capacity could gradually erode under climate warming in southern hemisphere EBUS (Humboldt and Benguela).

In major eastern boundary upwelling systems (EBUS), the spatiotemporal characteristics of MHWs, their generation mechanisms, and their biological impacts are now relatively well documented (Holbrook et al., 2019; Varela et al., 2021). In the California Current System (Northeast Pacific), MHWs mainly result from a weakening of upwelling-favorable winds, which reduces vertical cooling and favors the accumulation of heat at the surface, while compressing phytoplankton blooms toward the coast (Black et al., 2025). In the Humboldt-Peru system (Southeast Pacific), although the longest MHWs (>100 days) are associated with remote equatorial variability such as El Niño, the majority of events are driven by the relaxation of local coastal winds (Pietri et al., 2021). In the Benguela system (Southeast Atlantic), while upwelling plays a moderating role on coastal MHWs, recent projections indicate that both this system and the Humboldt are likely to become future MHW hotspots under anthropogenic warming, as the weakening of boundary currents gradually surpasses the buffering capacity of upwelling (Wang et al., 2023). Horizontal advection processes also contribute to the intensification of current events (Holbrook et al., 2019). Despite these regional variations, a common paradigm emerges: persistent cold-water upwelling zones act as relative thermal refuges, with lower trends in MHW frequency near the coast than in regions not influenced by upwelling (Varela et al., 2021). Bakun et al. (2015) further proposed that intensifying coastal upwelling under climate change could regionally buffer surface warming and nutrient declines, though this remains debated in tropical EBUS.

However, this thermal refuge paradigm is mainly based on studies of temperate EBUS, such as the California, Humboldt, and the northern part of the Canary Current systems, where upwelling intensity generally peaks in summer. It largely overlooks

https://doi.org/10.5194/egusphere-2026-2571
Preprint. Discussion started: 21 May 2026

tropical systems characterized by an opposite seasonality, in which upwelling reaches its maximum during the boreal winter. The Senegal-Mauritania Upwelling System (SMUS) is indeed one of the few tropical EBUS where coastal upwelling attains its highest intensity (November–May) in boreal winter/spring, under the combined influence of the Azores High and the meridional migration of the Intertropical Convergence Zone (ITCZ) (Faye et al., 2015; Ndoye et al., 2014; Cropper et al., 2014). During winter, the persistence of the northeast trade winds generates an offshore-directed Ekman transport, inducing the upwelling of cold, nutrient-rich waters that maintain anomalously low sea surface temperatures (SST) and sustain high coastal biological productivity (Lathuiliere et al., 2008; Sylla et al., 2019). Its sensitivity to thermal anomalies is nevertheless well documented: the so-called Dakar Niño/Niña (Oettli et al., 2016), recurrent positive SST anomalies between February and April, are regularly associated with episodes of low net primary production during the main upwelling season (Imbol Koungue et al., 2025). This winter dynamics, which would theoretically limit the frequency and intensity of MHWs, remains poorly studied.

This context of intense winter upwelling takes on particular significance for small pelagic populations that rely heavily on it, notably the round sardinella (Sardinella aurita). Studies by Mbaye et al. (2015) demonstrated that the recruitment success of these species depends on an optimal environmental window, in which upwelling intensity must provide sufficient nutrient enrichment without causing excessive larval dispersal offshore. The main spawning period, concentrated at the end of the cold season in the southern SMUS (November–April, Senegalese coasts) and during summer over the Banc d'Arguin (July–August), coincides precisely with critical oceanographic transitions (Boely et al., 1978; Zeeberg et al., 2008). The occurrence of MHWs during these sensitive phases could disrupt this biological synchrony (match/mismatch), either through direct thermal stress on larval stages leading to reduced reproductive success (Durant et al., 2019), or through modifications in food availability via a reduction in phytoplankton biomass (Guibourd de Luzinais et al., 2025; Li et al., 2024). These disruptions thus threaten the sustainability of a major fishery resource, representing between 1.7 and 2.5 million tons of annual small pelagic catches in the Northwest African region (Lakhnigue et al., 2019) and accounting for approximately 72% of total landings in Senegal (Deme et al., 2022). Beyond their direct impacts on marine ecosystems, marine heatwaves (MHWs) in the tropical Atlantic have also been associated with contrasting effects on West African rainfall. In particular, warming events in the Gulf of Guinea are linked to rainfall deficits north of 10°N (Sahelian region) and precipitation surpluses to the south (Koné et al., 2025). In this context, the SMUS, located at the interface of these climatic regimes, represents a key region for investigating the interactions between ocean thermal extremes and regional climate variability.

These observations raise a fundamental question in the SMUS: how do wind-driven upwelling dynamics and their seasonal modulation control the emergence and intensity of marine heatwaves in this tropical upwelling system, and what are their immediate consequences for phytoplankton biomass in ecologically and socioeconomically critical regions? To address this question, this study investigates the physical and biological dynamics of marine heatwaves in the SMUS over the period 1982–2024. We first provide a spatio-temporal characterization of MHWs based on the standardized detection framework of Hobday et al. (2016) applied to satellite observations. Then, are examined the seasonal and long-term variability in relation to upwelling intensity and wind atmospheric heat forcing. Finally, the associated chlorophyll-a responses to MHW are assessed in

https://doi.org/10.5194/egusphere-2026-2571
Preprint. Discussion started: 21 May 2026

key coastal zones, with particular attention to periods and regions of ecological sensitivity linked to small pelagic fish spawning grounds.

This integrated analysis allows to disentangle the role of seasonal upwelling modulation in shaping MHW dynamics and their biological impacts in a tropical eastern boundary upwelling system. By identifying the conditions under which thermal extremes coincide with significant reductions or increase in chlorophyll-a phytoplankton biomass, this study provides new insights into the coupling between physical forcing and ecosystem response in a highly productive but climate-sensitive marine region.

2 Data and methodology

2.1 Study area: The Senegal–Mauritanian Upwelling System

The Senegal–Mauritanian Upwelling System constitutes the southern part of the Canary Current Upwelling System. It extends along the northwest African coast between 10°N and 22°N (Fig. A1), encompassing the coastal waters of Mauritania, Senegal, The Gambia, and Guinea-Bissau, and extending westward toward the Cape Verde archipelago (Arístegui et al., 2009; Cropper et al., 2014; Demarcq, 2009). This tropical Atlantic coastal ecosystem is among the most productive in terms of primary production (Abrahams et al., 2021; Chavez and Messié, 2009; Lathuiliere et al., 2008) and plays a crucial role in supporting fisheries and the economies of West African countries. This high productivity is sustained by a continuous supply of nutrients through dynamic coastal upwelling, whose regimes vary spatially (Vázquez et al., 2023).

To further investigate this spatial heterogeneity, the coastal domain is subdivided into distinct subregions (Fig. 1c). The delimitation of the study subregions is based on the well-documented hydro-climatic structure of the SMUS, characterized by strong latitudinal heterogeneity in dynamical forcing as well as thermal and biogeochemical responses. This partition does not represent an arbitrary division of the coastal domain, but rather aims to isolate three contrasting dynamical upwelling regimes: (i) a quasi-permanent upwelling zone in the north (Cap Blanc, 20.8°–22°N), dominated by persistently cold conditions and strong and sustained upwelling-favorable winds; (ii) an intermediate transition zone (Grande Côte–Cap Timiris, hereafter referred to as 'Grande Côte', 14.8°–19.2°N), characterized by marked seasonal variability in both forcing and thermal conditions; and (iii) a seasonal upwelling zone in the south (Petite Côte, 12.5°–14.6°N), under stronger tropical influence and exhibiting a weaker and seasonally confined upwelling signal. The sectors located between 19.2°N and 20.8°N (Banc d'Arguin) and in the Bijagós Archipelago area (10.5°–12°N) are excluded from the regional analysis. This decision is supported by previous studies indicating that these areas are characterized by weak vertical velocities and reduced upwelling intensity (Faye et al., 2015).

The analysis of the 90th percentile threshold over the reference period 1982–2011 (Fig. A1a) reveals a pronounced latitudinal gradient, with maximum values (27.5–28 °C) in the southern part of the SMUS (10°N–12°N) and minimum values (<20.5 °C) near Cap Blanc (20°N–22°N). This distribution reflects the contrasting influence of the quasi-permanent upwelling north of 20°N, driven by trade winds and Ekman transport, and the presence of warmer tropical water masses to the south. Over the period 1982–2024, SST exhibits a widespread and statistically significant warming trend ($p < 0.05$) across most of the study area (Fig. A1b). The highest warming rates (0.5–0.6 °C decade^{-1}) are observed over the continental shelf, particularly in the

https://doi.org/10.5194/egusphere-2026-2571
Preprint. Discussion started: 21 May 2026

Banc d'Arguin and the Bijagós Islands. In contrast, the Mauritanian coast north of 20°N and the Petite Côte of Senegal show no significant trends, suggesting a local modulation by upwelling dynamics.

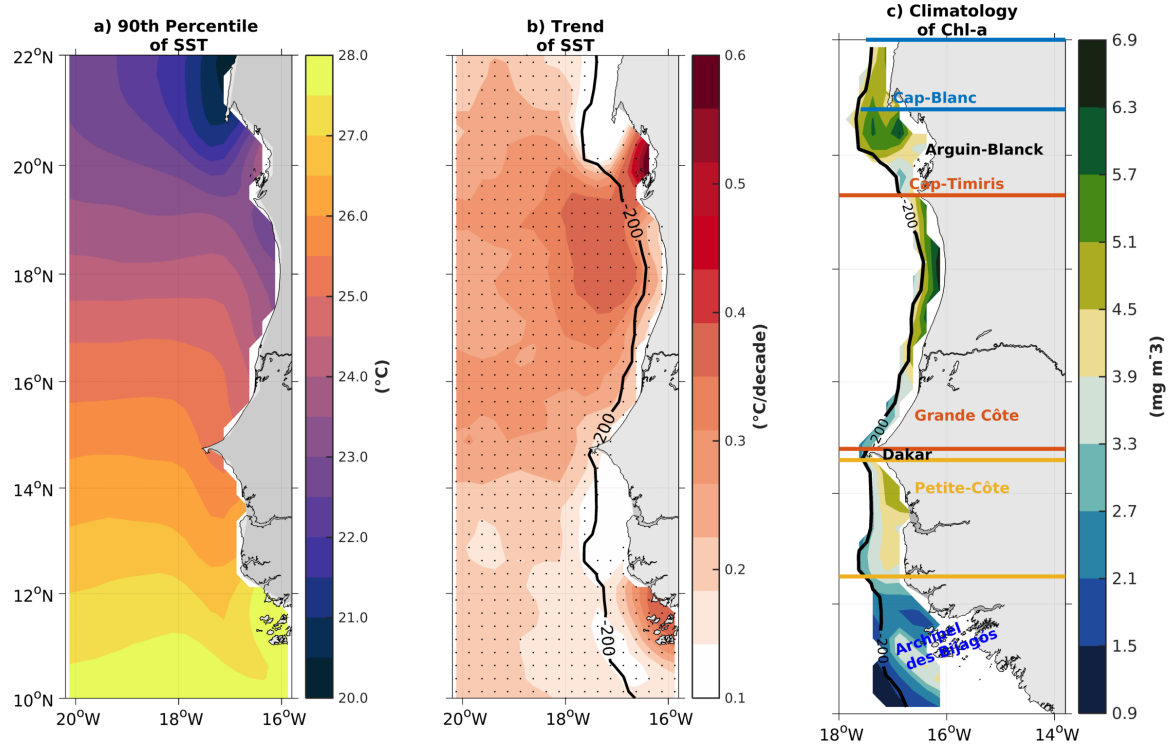

Figure 1. Hydro-climatic characterization of the SMUS upwelling system. (a) 90th percentile of sea surface temperature (SST (°C), 1982–2011), representing the upper thermal conditions of the reference climatology; (b) linear trend in SST (°C decade^{-1}, 1982–2024). Black dots indicate areas where trends are statistically significant (Mann–Kendall test, $p < 0.05$). The black contour denotes the 200 m isobath; (c) climatology of chlorophyll-a concentration (Chl-a, mg m^{-3}), used as a proxy for phytoplankton biomass and an indirect indicator of marine productivity. The three study subregions are defined latitudinally and delimited offshore by the 200 m isobath: Cap Blanc (20.8°–22°N), Grande Côte (14.8°–19.2°N), and Petite Côte (12.5°–14.6°N). These sectors were selected due to their pronounced upwelling dynamics (Faye et al., 2015) and their historical ecological importance as key areas for pelagic fish reproduction and fisheries resources (Boely et al., 1978).

2.2 Data

This study relies on three complementary datasets covering the period 1982–2024. SST data are derived from the NOAA Optimum Interpolation SST product (OISSTv2.1), which provides daily fields at a spatial resolution of 0.25°. This product combines observations from the Advanced Very High Resolution Radiometer (AVHRR) with in situ measurements (ships, buoys, and Argo floats) for bias correction (Reynolds et al., 2007). OISSTv2.1 is widely used for marine heatwave (MHW) analyses due to its continuous global coverage since 1982, temporal consistency, and its ability to capture synoptic-scale thermal extremes (Behr et al., 2025; Hobday et al., 2016; Oliver et al., 2018; Schlegel et al., 2021).

https://doi.org/10.5194/egusphere-2026-2571
Preprint. Discussion started: 21 May 2026

Phytoplankton biomass is estimated from daily chlorophyll-*a* concentrations (Chl-*a*, 4 km spatial resolution) obtained from the multi-sensor GlobColour product of the Copernicus Marine Service (CMEMS). This dataset covers the period 1998–2024 through the merging of observations from SeaWiFS, MODIS-Aqua, MERIS, VIIRS, and OLCI/Sentinel-3 sensors (Garnesson et al., 2019). The GlobColour product is particularly suitable for the analysis of upwelling systems due to its multi-sensor merging approach, which improves temporal coverage and chlorophyll retrieval in optically complex coastal waters, thereby reducing data gaps associated with frequent cloud cover in these regions (Maritorena and Siegel, 2005; Garnesson et al., 2019; Kahru et al., 2014).

Atmospheric and oceanic forcings are obtained from the ERA5 reanalysis produced by the European Centre for Medium-Range Weather Forecasts (ECMWF), which provides hourly fields of 10 m wind and net surface heat fluxes at a spatial resolution of 0.25° throughout the study period (Hersbach et al., 2020). The spatial and temporal consistency between OISSTv2.1 and ERA5, which share the same 0.25° resolution, facilitates the calculation of upwelling indices and the analysis of atmospheric forcings associated with MHWs. Physical analyses cover the entire 1982–2024 period, whereas the analysis of biological responses based on chlorophyll-*a* is limited to the satellite era (1998–2024). This constraint restricts the assessment of long-term biological trends but does not affect the characterization of the physical mechanisms driving MHWs. To ensure spatial consistency among the three datasets, ERA5 fields and GlobColour chlorophyll-*a* concentrations were interpolated onto the regular OISSTv2.1 grid (0.25° × 0.25°) using bilinear interpolation.

2.3 MHW definition and metrics

Marine heatwaves (MHWs) were detected and characterized using daily SST data from the OISSTv2.1 optimal interpolation product, following the standardized methodology of Hobday et al. (2016). An MHW is defined as a discrete and prolonged period during which daily SST exceeds a seasonally varying 90th percentile threshold for at least five consecutive days. Events separated by interruptions of up to two days are considered part of the same event. Climatological baselines and corresponding thresholds were calculated from daily SST data using an 11-day moving window centered on each calendar day over the 1982–2011 period (30 years). The choice of the 1982–2011 reference period is based on two key considerations. First, it satisfies the 30-year climatology requirement set by the World Meteorological Organization (WMO) and ensures comparability with previous MHW studies (Oliver et al., 2018; Smith et al., 2023). Second, it captures a complete cycle of Atlantic multidecadal variability, encompassing both the negative phase of the Atlantic Multidecadal Oscillation (AMO, 1982–1995) and the onset of its positive phase (1995–2011) (Enfield et al., 2001; Knight et al., 2005). Using a more recent climatology (1991–2020) would effectively normalize anomalies against a state already influenced by the positive phase of the AMO, thus underestimating the true amplitude of regional thermal changes and biasing the detection of contemporary extremes.

The use of a seasonal percentile, rather than a fixed threshold, allows thermal extremes to be identified relative to the local temperature regime and seasonal variability of each region. This approach is particularly suited for detecting ecologically relevant anomalies in highly seasonal systems such as the SMUS (Hobday et al., 2016; Frölicher and Laufkötter, 2018; Smith et al., 2023). Consequently, a temperature extreme in winter may not be extreme in summer, ensuring consistent event detection

https://doi.org/10.5194/egusphere-2026-2571
Preprint. Discussion started: 21 May 2026

throughout the year. Moreover, it is important to note that the reference period (1982–2011) is used solely to define the climatological threshold, whereas the analysis of trends and spatio-temporal evolution is conducted over the full study period (1982–2024). This distinction, which is standard in the literature (Oliver et al., 2018; Smith et al., 2023), allows recent changes to be assessed objectively relative to a stable climatology, rather than against a threshold that is itself affected by anthropogenic warming.

2.4 Diagnostic of local ocean–atmosphere conditions

To characterize the atmospheric and oceanographic conditions associated with marine heatwaves in the SMUS, two complementary diagnostic indices are used: the Ekman pumping velocity, which represents wind-driven circulation and coastal upwelling variability 2.4.1, and the Coastal Upwelling Index, which quantifies the thermal contrast between coastal and offshore waters as a proxy for upwelling intensity 2.4.2. These indices are complemented by the analysis of net heat flux (Q_{net}) and its components to describe air–sea heat exchange conditions during MHW events.

2.4.1 Calculation of Ekman pumping velocity

The Ekman pumping velocity (EPV) was estimated following classical Ekman theory (Ekman, 1905). Wind stress was first computed from the 10 m wind velocity using the standard bulk formulation (Large and Pond, 1981):

$$\boldsymbol{\tau} = \rho_a C_d |\mathbf{U}_{10}| \mathbf{U}_{10} \tag{1}$$

where $\rho_a = 1.225$ kg m^{-3} is the air density, $C_d = 1.25 \times 10^{-3}$ is the drag coefficient, and $\mathbf{U}_{10}$ is the wind vector at 10 m above the sea surface.

The horizontal divergence of Ekman transport induces a vertical velocity at the base of the Ekman layer, calculated from the wind stress curl (Bakun, 1973; Sylla et al., 2022):

$$EPV = \frac{1}{\rho_w f}\left(\frac{\partial \tau_y}{\partial x} - \frac{\partial \tau_x}{\partial y}\right) \tag{2}$$

where τ_x and τ_y are the zonal and meridional components of the wind stress (N m^{-2}), respectively, $\rho_w = 1025$ kg m^{-3} is the seawater density, and $f = 2\Omega \sin\phi$ is the Coriolis parameter, with $\Omega = 7.292 \times 10^{-5}$ rad s^{-1} the Earth's angular velocity and ϕ the geographic latitude.

EPV is expressed in m s^{-1}, where positive values indicate upwelling (upward motion of cold subsurface waters), whereas negative values correspond to downwelling (downward displacement of surface waters). Spatial derivatives were computed using centered finite differences on the regular ERA5 grid with a spatial resolution of 0.25°. This approach, widely used to characterize coastal upwelling intensity in eastern boundary systems (Bakun, 1973; Pickett and Paduan, 2003), has been successfully applied in the Northeast Atlantic (Cropper et al., 2014) and specifically in the SMUS (Sylla et al., 2022).

https://doi.org/10.5194/egusphere-2026-2571
Preprint. Discussion started: 21 May 2026

2.4.2 Thermal Coastal Upwelling Index

The intensity of coastal upwelling was estimated using the Coastal Upwelling Index (CUI), defined as the SST difference between an offshore oceanic region and a coastal region influenced by upwelling (Demarcq, 2009; Benazzouz et al., 2014; Sylla et al., 2022):

$$CUI = SST_{offshore} - SST_{coast} \tag{3}$$

where SSTcoast corresponds to the SST in the immediate vicinity of the coastline, and SSToffshore to that measured offshore at a distance of 5° longitude westward from the coast, in accordance with approaches commonly used in the literature (Cropper et al., 2014; Sylla et al., 2022). High positive values indicate intense upwelling, whereas low or negative values indicate a weakening or relaxation of upwelling (Fig. A1a). In the SMUS, this index has been widely used to characterize the spatio-temporal variability of thermal upwelling, particularly at seasonal and interannual scales.

2.5 Statistical Analysis Methods

Several statistical methods were employed to analyze temporal trends, characterize the atmospheric and oceanic signatures of MHWs, and quantify the phytoplankton biomass response.

2.5.1 Long-term Trend Analysis

Temporal trends in MHW characteristics (Days, duration, maximum intensity) over the period 1982–2024 were estimated using the non-parametric Mann-Kendall test (Mann, 1945; Kendall, 1975), which is suitable for environmental time series with non-normal distributions. Trend magnitudes were quantified using Sen's slope estimator (Sen, 1968), based on the median of slopes between pairs of observations and robust to outliers. Statistical significance was assessed at $\alpha = 0.05$ (95% confidence level). These analyses were conducted at the regional scale, using spatial averages over the three subregions (squares in Fig. 1c), as well as at each grid point to identify areas with significant changes. This methodological approach is consistent with recent studies documenting the global increase in MHWs over the past decades (Oliver et al., 2018).

2.5.2 Composite Analysis of Physical Forcings

To characterize the physical forcings associated with MHWs, composite analyses were performed on all detected events (1982–2024) within the three subregions (Fig. 1c). The composite approach is widely used to identify MHW drivers, particularly in tropical regions where interactions between local forcings and climate teleconnections are complex. Recently, Ningsih et al. (2025) applied this method to analyze MHW impacts on upwelling in southern Java, highlighting the role of heat advection and air-sea fluxes. Similarly, Yu et al. (2025) used composites to classify different MHW types in the western Indian Ocean, demonstrating that the suppression of evaporative cooling (positive latent heat flux) is a key mechanism, especially in upwelling regions.

https://doi.org/10.5194/egusphere-2026-2571
Preprint. Discussion started: 21 May 2026

Anomalies in SST, winds, heat fluxes, EPV, and CUI were computed by subtracting the seasonally smoothed climatology (1982–2011) using an 11-day running window, followed by a 30-day low-pass filter to remove high-frequency variability. For each event, the onset day was defined as day 0, and a ±30-day window was extracted around it (61 days total). The anomalies were then averaged across all events to obtain a typical composite signature.

In this study, the characterization of physical regimes associated with MHWs relies on a composite-based approach combining anomalies of net heat flux (Q_{net}), the CUI, and the EPV. This approach does not constitute a full mixed-layer heat budget, but rather aims to identify consistent signatures of thermodynamic (air–sea heat fluxes) and dynamic (upwelling- and wind-driven) contributions. Within this framework, CUI and EPV are used as complementary proxies of the variability of dynamic processes, reflecting the intensity of coastal upwelling and the effects of large-scale wind-driven Ekman pumping, respectively. However, they do not represent the full range of residual oceanic processes (such as horizontal advection or vertical mixing), which are not explicitly quantified here.

2.5.3 Analysis of Phytoplankton Response

To assess the impact of MHWs on phytoplankton biomass, similar composite analyses were performed on chlorophyll-a anomalies over the satellite period 1998–2024. The full period was used to compute the seasonal climatology and detect MHW events. In addition to temporal composites (±30 days), spatial composites were calculated by averaging anomalies over the entire duration of each event (from onset to termination), revealing the typical spatial distribution of the biological impact.

3 Results and discussion

3.1 Spatial distribution of MHW characteristics

3.1.1 Climatological mean patterns

The spatial distribution of mean MHW characteristics over the 1982–2024 period shows strong spatial variability within the SMUS (Fig. 2). The spatial pattern of annual MHW days (Fig. 2a) exhibits marked regional contrasts. The highest values (around 50 days yr^{-1}) are located over the two very shallow areas in the Banc d'Arguin (20°N) and the Bijagós archipelago area (10.5°–12°N). These two sub-regions are characterized both by weak vertical velocities leading to an inhibition of upwelling (Faye et al., 2015, Fig. A1) and by the strongest SST warming trends in the domain (about 0.5 °C $decade^{-1}$; Fig. 1b), these two combined factors could explain their particularly high number of MHW days. A large offshore area (beyond the continental shelf) between 16°N and 20°N exhibits elevated values of MHW days, around 40 days yr^{-1}. This region is primarily characterized by a significant SST warming (Fig. 1b). This relationship between surface warming and MHW occurrence is consistent with the findings of Oliver et al. (2018), who showed that the increase in the annual number of MHW days is largely explained by the rise in mean ocean temperature.

In contrast, the lowest values of the annual number of MHW days, ranging from about 20 to 30 days, are observed in Cap Blanc and the Petite Côte, and coincide with areas where upwelling is strongest and most seasonally persistent. This

https://doi.org/10.5194/egusphere-2026-2571
Preprint. Discussion started: 21 May 2026

overall correspondence between upwelling and the total numbers of MHW days is consistent with previous studies showing that upwelling systems act as thermal refugia, moderating regional warming (Varela et al., 2021; Seabra et al., 2019), through the upwelling of subsurface waters. The mere presence of cold waters upwelled near the coast therefore appears sufficient to reduce the number of MHW days compared to adjacent offshore areas less influenced by this process.

Regarding the mean duration of MHWs, it ranges approximately from 9 to 20 days (Fig. 2b). The most persistent events predominate offshore, with maxima located between 16°N and 19°N (18 to 20 days), whereas shorter durations (< 15 days) characterize the continental shelf, with minima reaching about 9 days. The frequency of MHWs (Fig. A6a) shows spatial variability similar to that of the annual number of MHW days (Fig. 2a). It ranges between 1 and 3 events per year, with low occurrences in the upwelling regions of Cap Blanc and the Senegalese Petite Côte. This distribution suggests that upwelling regions, characterized by the presence of recently upwelled waters that are less warmed by human activities, are associated with events that are both less frequent and shorter in duration. The thermal properties of these waters thus play a key role in controlling these temporal characteristics at the regional scale.

Maximum intensity (Fig. 2c), a pronounced coast–offshore gradient is highlighted, with values ranging between 3.0 and 3.5 °C over the continental shelf and between 2.0 and 2.5 °C in the open ocean. However, we interpret this general pattern not as being related to the thermal properties of upwelled waters, but rather to the intense dynamics of coastal upwelling. Indeed, these intensity peaks spatially coincide with regions of strong horizontal SST gradients (Fig. 2c, contours), characteristic of thermal fronts generated by the upwelling system. These fronts, in the presence of intensified shelf currents (not shown; see Faye et al. (2015), are associated with stronger heat advection and, consequently, with larger SST anomalies. This correspondence highlights the key role of frontal dynamics in modulating the extreme intensity of MHWs. It can be largely explained by the thermal stratification induced by coastal upwelling: the upwelled cold waters maintain a relatively low background temperature along the coast, so that when a MHW occurs, the thermal anomaly defined relative to this cold climatology can reach high values even if absolute temperatures remain moderate. This mechanism, already documented in other eastern boundary upwelling systems, notably in the California Current System (Jacox et al., 2020), highlights the role of background thermal contrast in the apparent amplification of event intensity. In addition, as highlighted by Holbrook et al. (2019), local processes within the mixed layer, including strong frontal gradients and mesoscale variability, are key modulators of MHW characteristics, enhancing event intensity along the coast.

In summary, the analysis of annual means reveals a contrasted spatial organization of MHWs across the SMUS. The highest values of the annual number of MHW days (40 to 52 days yr^{-1}) occur in two distinct contexts: first, in shallow regions without upwelling (Banc d'Arguin, Bijagós), where the absence of cold water upwelling suppresses vertical cooling; and second, in the oceanic region between 16°N and 20°N, where strong SST warming (Fig. 1b) promotes heat accumulation at the surface. Conversely, regions of intense permanent or seasonal upwelling (Cap Blanc, Petite Côte) exhibit the lowest values (20 to 30 days yr^{-1}). Mean duration is shorter over the continental shelf (∼10 days) than offshore, while maximum intensity follows a pronounced coast–offshore gradient (3.0–3.5 °C over the shelf versus 2.0–2.5 °C offshore).

https://doi.org/10.5194/egusphere-2026-2571
Preprint. Discussion started: 21 May 2026

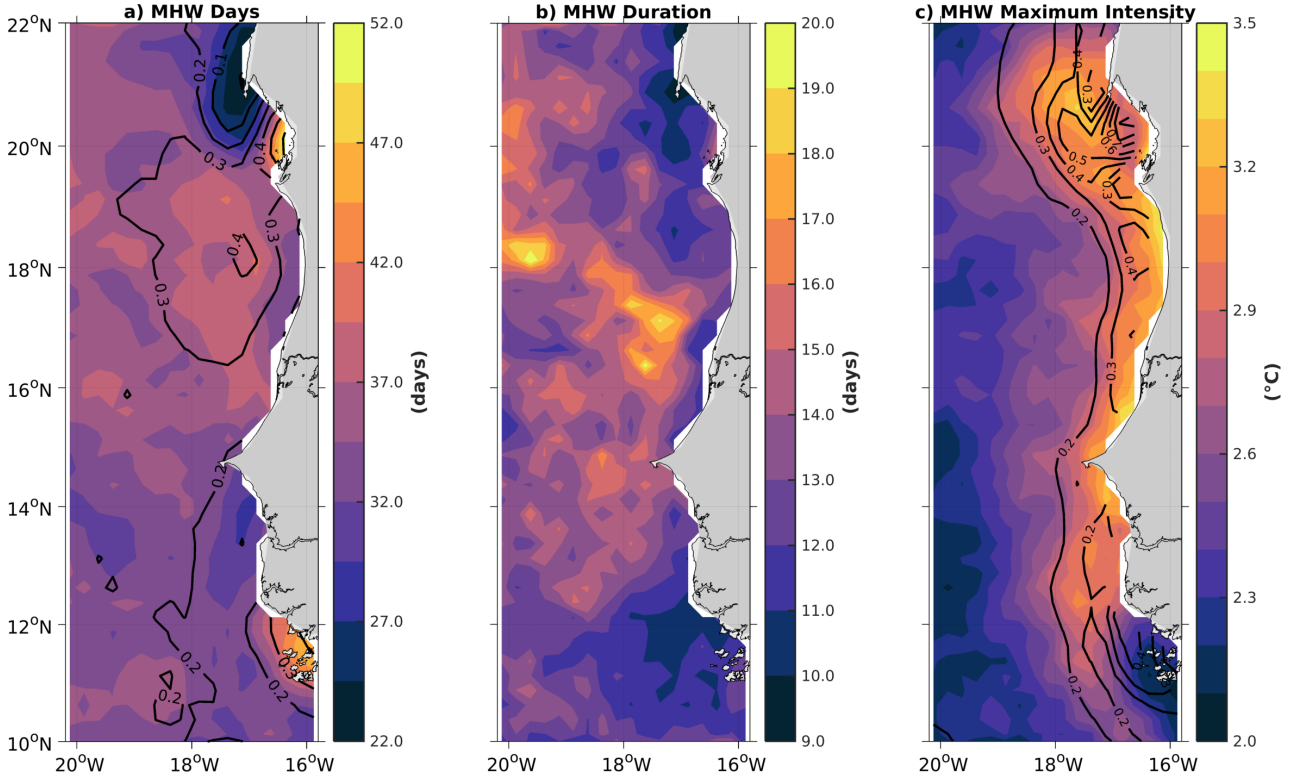

Figure 2. Spatial distribution of mean annual marine heatwave (MHW) characteristics in the SMUS (1982–2024): a) total number days per year, b) duration (days), and c) maximum intensity (°C). Black contours in a show the linear SST trends (°C decade^{-1}), while contours in c depict the spatial gradient norm of SST.

3.1.2 Seasonal variability

The seasonality of MHWs in the SMUS is examined by classifying each event according to the season during which its maximum intensity is reached. The two seasons defined by Faye et al. (2015) are used: the cooling period (CP: November–May) and the warming period (WP: June–October). This approach highlights a marked seasonal contrast in MHW characteristics.

MHW activity is significantly higher during the CP than during the WP, with a particularly pronounced contrast south of 18°N, where seasonality is strong, both over the continental shelf and in the open ocean (Faye et al., 2015). During the CP, the number of MHW days reaches up to 30 days yr^{-1} offshore and about 25 days yr^{-1} over the continental shelf (Fig. 3a1), corresponding to approximately three and two times higher values, respectively, than during the WP (Fig. 3a2). The highest coastal values are again found in the two sub-regions of the Banc d'Arguin and the Bijagós. In contrast, the WP is characterized by a low occurrence of MHWs across the entire domain, with values rarely exceeding 16 days yr^{-1}. The mean duration of events, which is the main contributor to the total annual number of MHW days, is also longer during the CP south of 18°N, by a factor close to two, although the range of values is similar between seasons (8–26 days; (Figs. 3b1-2).

https://doi.org/10.5194/egusphere-2026-2571
Preprint. Discussion started: 21 May 2026

In contrast to occurrence and duration, whose spatial distributions appear highly heterogeneous, maximum MHW intensity exhibits a more coherent regional structure. The seasonal analysis reveals a marked reversal of the dominant spatial gradient. During the CP, the strongest thermal anomalies (2.5–3.0 °C) are concentrated along the coastal band between 12°N and 19°N (Fig. 3c1). During the WP, this gradient weakens and reorganizes along a north–south axis: the highest intensities (2.8–3.2 °C) shift toward the Cap Blanc region (19–22°N), whereas the southern sector (below 14°N) exhibits the lowest values (1.4–1.8 °C; Fig. 3c2), following the northward migration of the upwelling front (Diakhaté et al., 2016). Thus, as for the annual mean discussed in the previous section, MHW occurrence primarily reflects the general SST warming trend (Oliver et al., 2018), whereas maximum intensity appears to be governed by upwelling dynamics: the most intense MHWs occur in regions with the lowest SST, and the seasonal reversal of the spatial gradient reflects a seasonal reconfiguration of coastal upwelling.

https://doi.org/10.5194/egusphere-2026-2571
Preprint. Discussion started: 21 May 2026

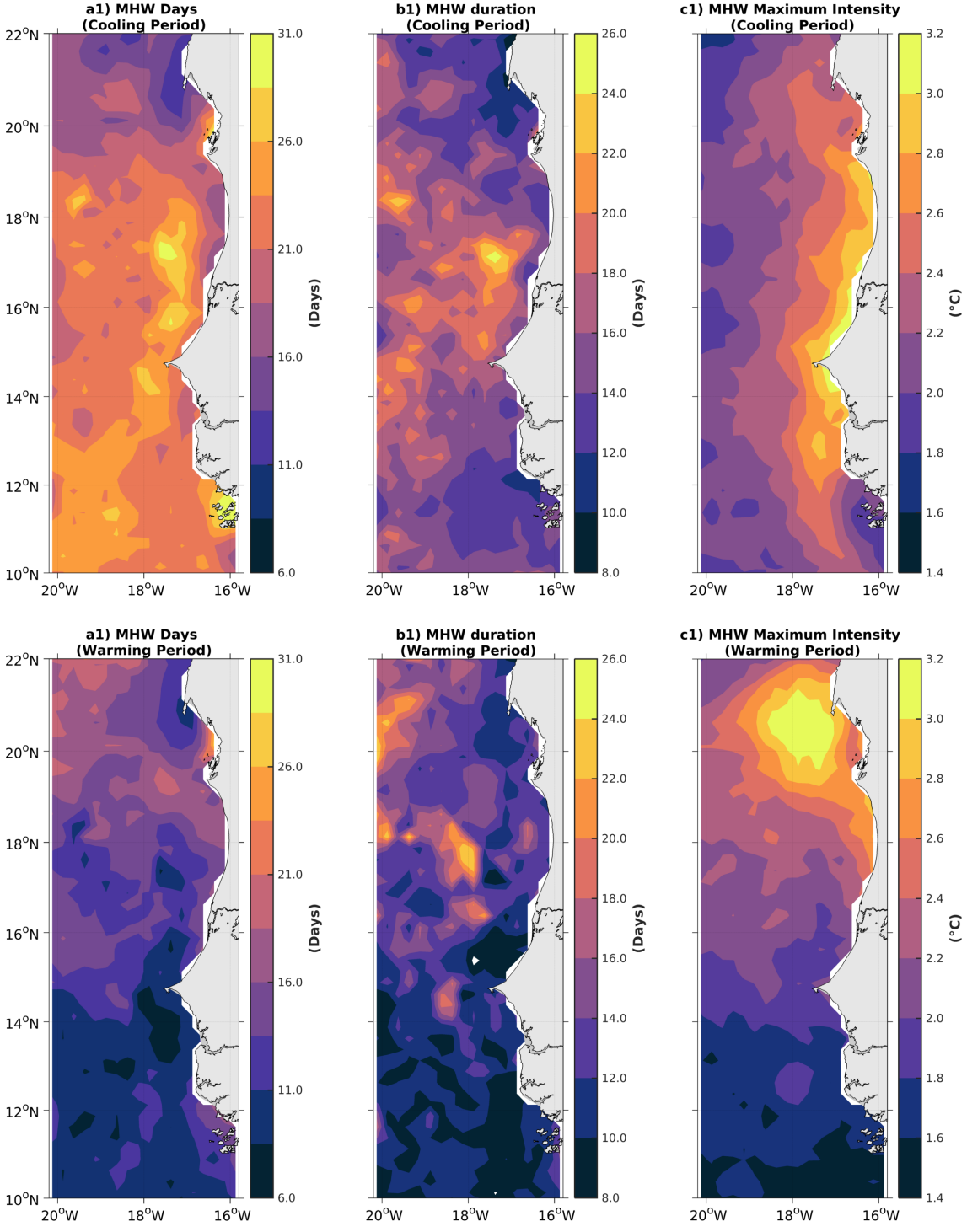

Figure 3. Spatial distribution of the seasonal mean characteristics of marine heatwaves (MHWs) in the SMUS over the period 1982–2024. (a1–a2) total number of MHW days per year, (b1–b2) mean duration (days), and (c1–c2) maximum intensity (°C). Subscripts 1 and 2 refer to the cooling (November–May) and warming (June–October) periods, respectively.

https://doi.org/10.5194/egusphere-2026-2571
Preprint. Discussion started: 21 May 2026

Table 1. Characteristics of marine heatwaves (MHWs) in the three SMUS sub-regions (1982–2024) for the whole year and by season.

Sub-region	Period	No. of MHW	Cumulative days	Mean duration (days)	Max. intensity (°C)
Cap Blanc (20–22°N)	Annual	92	1171	12.73	2.31
	Cooling (Nov–May)	53	674	12.72	2.10
	Warming (Jun–Oct)	39	497	12.74	**2.60**
Grande Côte (14.8–19.2°N)	Annual	102	**1654**	16.22	2.31
	Cooling (Nov–May)	47	937	**19.94**	**2.63**
	Warming (Jun–Oct)	55	717	13.04	2.04
Petite Côte (12.5–14.6°N)	Annual	89	1357	15.25	2.28
	Cooling (Nov–May)	58	973	16.78	**2.65**
	Warming (Jun–Oct)	31	384	12.39	1.57

Table 1 highlights a clear regional signature of MHW characteristics. The Grande Côte region concentrates the highest MHW activity (102 events and 1654 cumulative days), the Petite Côte exhibits the strongest intensities during the CP (2.65 °C), whereas Cap Blanc is characterized by a remarkably stable mean duration (12.7 days) and reaches its maximum intensity during the WP (2.60 °C).

3.2 Long-term spatio-temporal trends

3.2.1 Spatial distribution of linear trends inof MHW metrics

Figure 4 presents long-term linear trends (1982–2024) in the annual total number of MHW days, duration, and maximum intensity in the SMUS. The first two characteristics exhibit statistically significant increasing trends at the 95% confidence level (Figs. 4a-b), interestingly unlike maximum intensity. The total number of MHW days increases by up to 30 days decade^{-1} across the domain, with the highest values concentrated over the Banc d'Arguin shelf and the Bijagós Archipelago (regions where thermodynamics are not driven by upwelling physics). More moderate increases (5–10 days decade^{-1}) are observed along the Senegalese coast, whereas trends are very weak or absent (non-significant) along the Mauritanian coast north of 20°N, particularly in the Cap Blanc region. In contrast, the mean duration reaches significant trends locally of 5 days decade^{-1}, with a more heterogeneous spatial distribution and no clearly defined coastal–offshore or meridional gradient. Elevated values are mainly scattered between 14°N and 19°N especially along the coast.

Unlike the trends observed for the total number of MHW days and duration, the trend in maximum intensity is not significant over most of the SMUS. It displays both positive and negative tendencies, ranging from -0.20 to $0.20\,^{\circ}$C decade^{-1}. Positive trends are mainly located north of 18°N, reaching a maximum of $0.20\,^{\circ}$C decade^{-1}, whereas negative trends occur south of 15°N (Fig 4c).

The Cap Blanc near-coast region (21–22°N) represents a remarkable singularity, being the only area where trends in total number of MHW days, duration, and maximum intensity generally do not reach statistical significance.

https://doi.org/10.5194/egusphere-2026-2571
Preprint. Discussion started: 21 May 2026

This relative stability of MHW indicators, despite ongoing global warming, accounts for the efficiency of local upwelling processes to mitigate the quantity of heat in extreme events. Similarly, the seasonal upwelling region of southern Senegal (12-15°N) also exhibits very weak increases in total number of MHW days and duration.

Overall, these findings support the idea that the coastal upwelling system mitigates the impacts of global warming on marine heatwaves. This is consistent with previous studies in other eastern boundary upwelling systems, such as the Benguela and Canary Current systems (Seabra et al., 2019; Varela et al., 2021), which report weaker MHW trends in upwelling-dominated coastal regions compared to adjacent offshore waters.

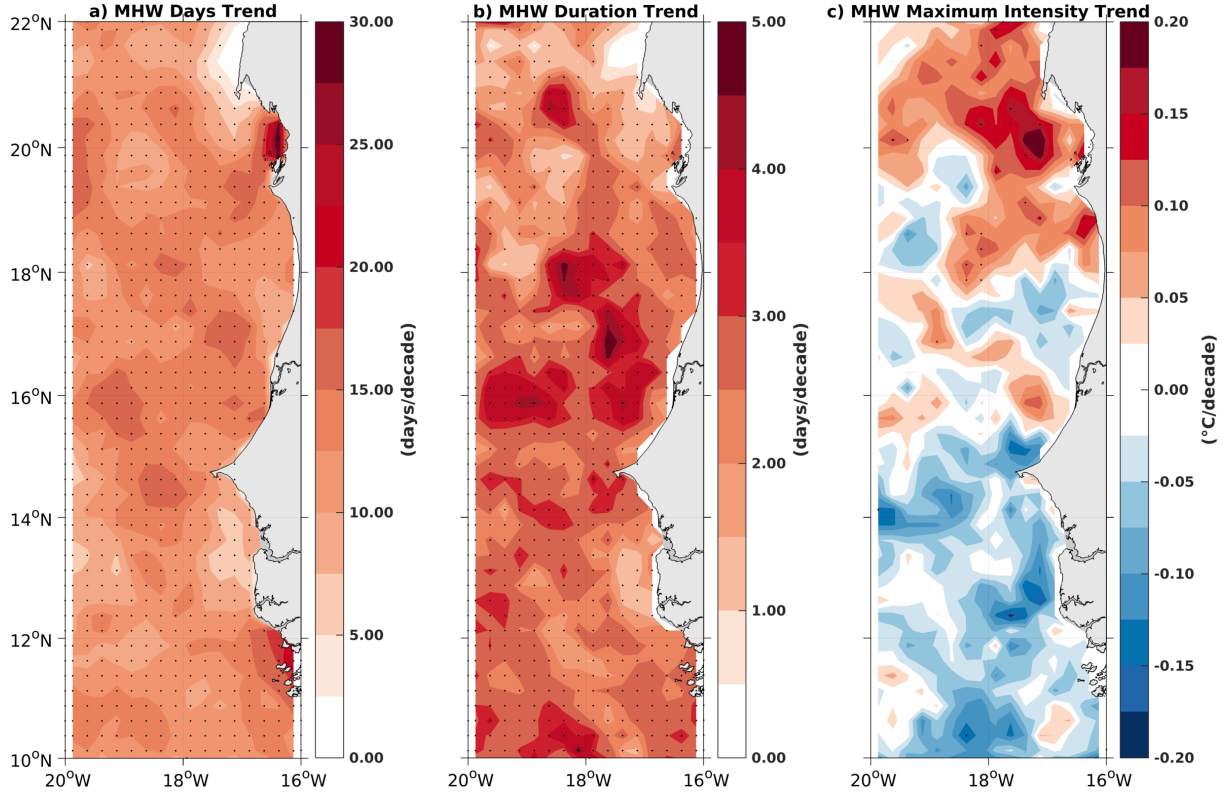

Figure 4. Long-term trends in marine heatwave (MHW) characteristics in the Senegal–Mauritania coastal upwelling system over the period 1982–2024: a) total number of MHW days per year (days decade^{-1}), b) mean duration (days decade^{-1}), and c) maximum intensity (°C decade^{-1}). Black dots indicate areas where the trend is statistically significant at the 95% confidence level ($p < 0.05$).

To evaluate the seasonality of these trends, we computed them for CP and WP (Fig. 5). The results indicate that the sign of the trends remains stable for the three characteristics, whereas their magnitude exhibits major contrasts. For both days and duration, trends are overall stronger, by about a factor of two, during the CP, with frequencies ranging from 2 to 12 days decade^{-1} and highest values still concentrated within the Banc d'Arguin and Bijagós Archipelago. A few areas show near-zero trends, mainly along the Mauritanian coast, north of 20°N (Cap Blanc region). The duration trend during the CP reaches rates of up to +9 days decade^{-1}, with maxima located in the same open ocean sector (14°N–19°N). These values highlight that the

https://doi.org/10.5194/egusphere-2026-2571
Preprint. Discussion started: 21 May 2026

long-term intensification of MHW parameters is primarily concentrated during the cold season. Regarding maximum intensity, results are again statistically insignificant.

In summary, the Grande Côte area concentrates the strongest trends in total number of MHW days and duration, particularly during the CP, whereas Cap Blanc is characterized by relative stability of all indicators. The Petite Côte shows an intermediate situation, with significant but moderate trends.

Let us now look at the same three characteristics in annual mean, but spatially averages in each three sub-regions,in the form of linear trend and interannual time-series.

https://doi.org/10.5194/egusphere-2026-2571
Preprint. Discussion started: 21 May 2026

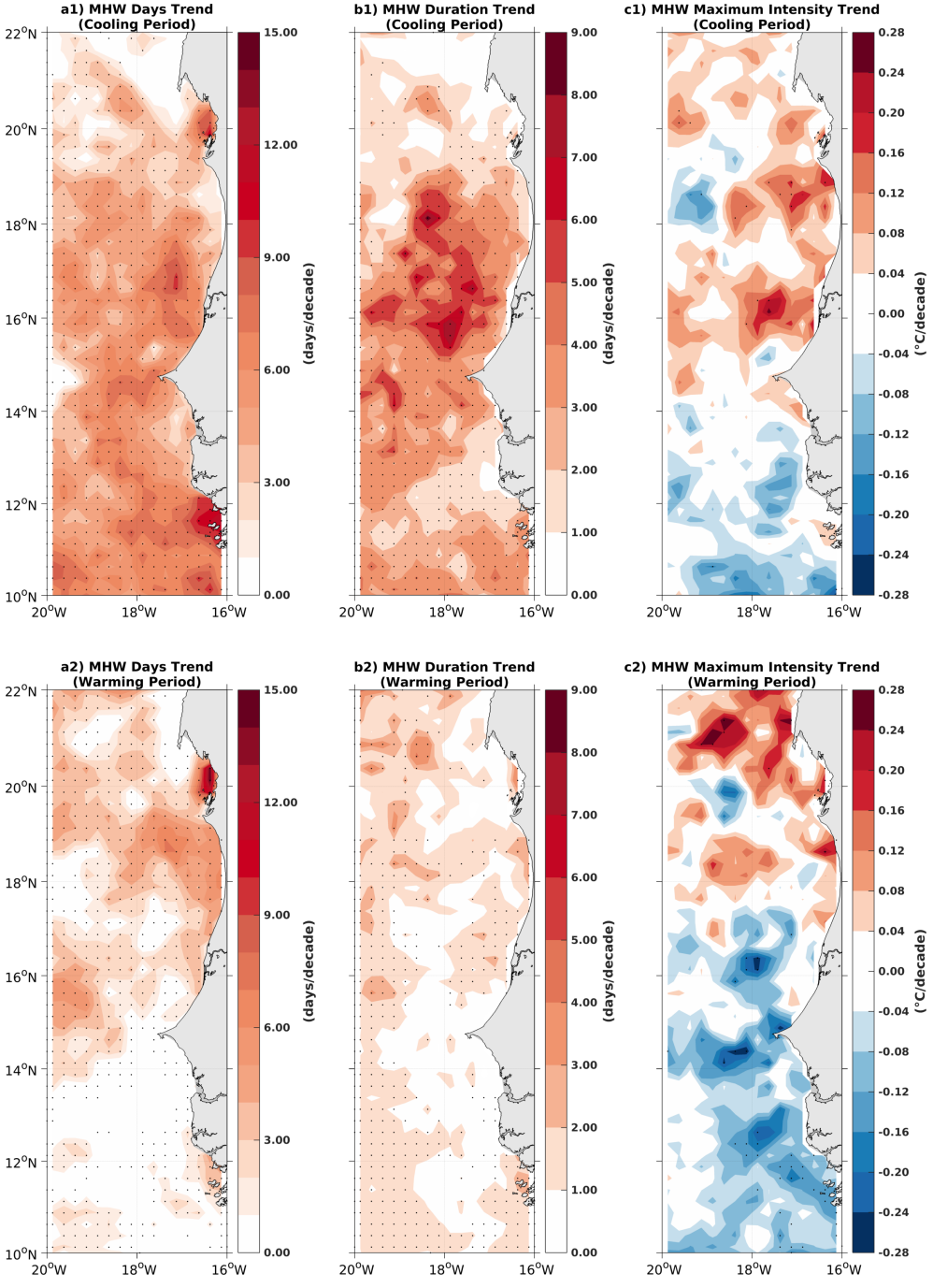

Figure 5. Seasonal spatial trends in marine heatwave (MHW) characteristics in the SMUS (1982–2024), for the CP and the WP. Panels (a1–c1) and (a2–c2) correspond to these two seasons, respectively. Columns show: (a) total MHW days (days decade^{-1}), (b) mean duration (days decade^{-1}), and (c) maximum intensity (°C decade^{-1}). Black dots indicate statistically significant trends ($p < 0.05$, Mann–Kendall test).

https://doi.org/10.5194/egusphere-2026-2571
Preprint. Discussion started: 21 May 2026

3.2.2 Interannual variability and linear trends in the three key sub-regions

Interannual variability, as well as the above long-term trends, are displayed in (Fig. 6) for the three coastal sub-regions Cap Blanc, Grande Côte, and the Petite Côte (delineated in Fig. 1c). A clear intensification in both the frequency and mean duration of MHWs is observed across all three sub-regions. The Grande Côte region exhibits the strongest and statistically significant positive trends, with an increase of about 10.25 days decade^{-1} in the total annual number of MHW days (Fig. 6a2) and 2.22 days decade^{-1} in mean duration (Fig. 6b2). Positive, though less pronounced, trends are also visible in the other sub-regions : the annual number of MHW days increases by 8.70 days decade^{-1} along the Petite Côte and by 4.35 days decade^{-1} at Cap Blanc. These results highlight the heightened vulnerability of the Grande Côte sector. With respect to event duration, the Grande Côte and Petite Côte regions exhibit trends of about 2 days decade^{-1}, whereas no significant trend is observed at Cap Blanc. Regarding maximum intensity, no significant trend is observed, but in the Grande Côte region, maximum intensity increases by 0.16 °C decade $^{-1}$ during WP (Fig. A5c2), while remaining stable during CP.

We now turn to the study of interannual variations. All examined metrics display strong interannual variability, punctuated by several extreme events. The years 1998, 2010, 2015–2016, 2019–2020, and 2022–2023 stand out for their exceptionally high values. The peak observed in 2023, reaching 180 cumulative MHW days in both the Petite Côte and the Grande Côte, represents the most extreme event over the entire 1982–2024 period. The overall patterns seem to present an intensification in MHW activity near the begining of the 21th century. coinciding with the transition of the Atlantic Multidecadal Oscillation (AMO) to a positive phase. This suggests a combined forcing by natural and anthropogenic warming, Note also the possible inprint of the 2023–2024 El Niño event. Overall, the results emphasize that while global ocean warming drives the general increase in MHW occurrence and duration, regional processes, particularly coastal upwelling play a crucial role in modulating their spatial distribution, seasonal expression, and long-term evolution.

https://doi.org/10.5194/egusphere-2026-2571
Preprint. Discussion started: 21 May 2026

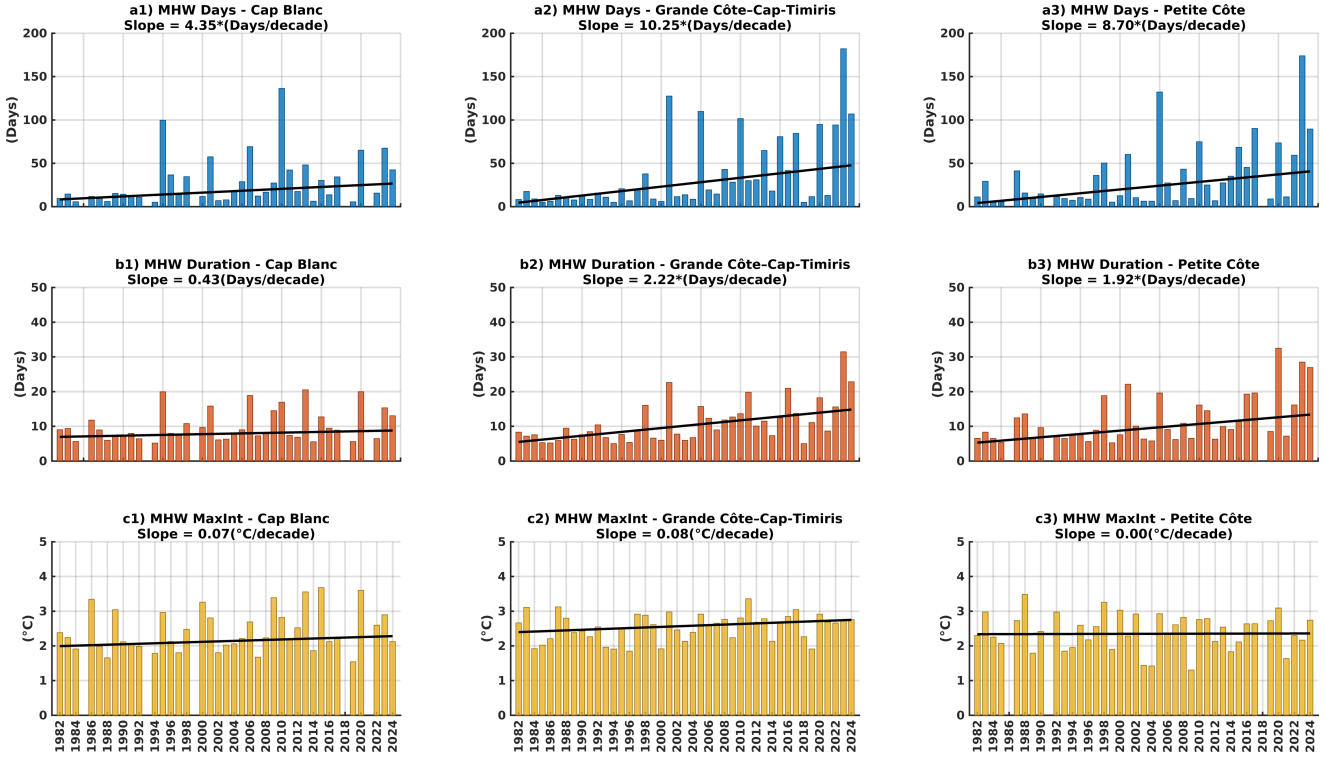

Figure 6. Interannual variability and long-term trends of marine heatwaves (MHWs) in the three SMUS sub-regions over the 1982–2024 period. Columns correspond to sub-regions: (1) Cap Blanc, (2) Grande Côte, and (3) Petite Côte. Rows represent different MHW characteristics: a) total annual number of MHW days (blue), b) mean event duration (days, orange), and c) maximum intensity (°C, yellow). Solid black lines represent linear trends estimated using Sen's slope method. Reported values indicate the decadal rate of change for each sub-region. The asterisk (*) denotes statistical significance at the 95% confidence level ($p < 0.05$, Mann–Kendall test).

Table 2. Long-term linear trends (1982–2024) of MHW characteristics in the three sub-regions of the SMUS, by season. Trends are estimated using the Mann-Kendall test and Sen's slope estimator. Asterisks (*) indicate a significant trend at the 95% confidence level ($p < 0.05$).

Sub-region	Period	Cumulative (days/decade)	Mean duration (days/decade)	Max. intensity (°C/decade)
Cap Blanc (20–22°N)	Annual	+4.35*	+0.43	+0.07
	Cooling (Nov–May)	+1.41	+0.40	+0.00
	Warming (Jun–Oct)	+1.94	+0.43	+0.19
Grande-Côte (14.8–19.2°N)	Annual	**+10.25***	**+2.22***	+0.08
	Cooling (Nov–May)	+6.75*	+2.35*	+0.14
	Warming (Jun–Oct)	+6.00*	+2.64*	**+0.16***
Petite-Côte (12.5–14.6°N)	Annual	+8.70*	+1.92*	0.00
	Cooling (Nov–May)	+5.16*	+2.3*	0.00
	Warming (Jun–Oct)	+1.34	+0.72*	-0.00

https://doi.org/10.5194/egusphere-2026-2571
Preprint. Discussion started: 21 May 2026

3.3 Atmospheric conditions and upwelling response during MHWs

In this section, we present a 61-day composite analysis of the main forcings associated with MHWs in each of the three sub-coastal regions.

3.3.1 Composite analysis over all events

The local physical processes controlling the initiation, intensification, and decay of MHWs in the SMUS were diagnosed using a composite analysis of all events detected between 1982 and 2024 across the three sub-coastal regions. Each event was centered on its initiation day (J0) and analyzed over a ±30-days window, allowing a detailed characterization of the forcings during the preconditioning, peak and dissipation phases of the extremes. Figure 7a displays three SST peaks of about equal intensities of 1.7 to 1.9 °C. The MHWs develop in a sudden final increase of near 1°C over 2-3 days from anomalously warm preconditions of +0.5 to +0.9°C, and then dissipates over a almost 10 times longer duration of 20 days, before returning to initial warm preconditions. The forcing intensity is strongly region-dependent, reflecting differences in upwelling system functioning.

During the preconditioning phase (J-30 to J0), all sub-coastal regions exhibit a weakening of trade winds, which drastically intensifies in the final 5 to 10 days prior to onset (-1.5 to -2.73 m s^{-1}; Fig. 7c), and quasi symmetrically vanishes over the same number of days. This 20-day wind relaxation pulse reduces wind stress (not shown), and its curl as shown by Ekman pumping (EPV; Fig. 7d), thereby weakening the whole range of upwelling processes, namely horizontal and vertical advection and mixing of colder water. The EPV anomalies of $0.2–0.4 \times 10^{-5}$ m s^{-1} represent about 10% of the climatological values in the region (Faye et al., 2015). This wind relaxation pulse is consistent with large-scale atmospheric reorganizations documented in the broader North Atlantic domain, where weakening of the Azores High associated with specific teleconnection patterns has been shown to suppress trade winds, modify air–sea heat fluxes, and promote stratification, ultimately driving sustained surface warming (Behr et al., 2025).

The air-sea net heat budget flux reaches values of +10 to +20 W m^{-2} during a few days (Qnet ; Fig. 7b) and comparable negative values afterwards. A gross heat budget calculation for a typical 20 m depth mixed layer (Faye et al., 2015), shows that the net heat flux warms the SST by of a few tenth of degrees only, suggesting a dominant role of oceanic heat fluxes in these three regions of upwelling. Model study of wind pulse in the senegalese upwelling by (Chabert et al., 2023), for comparable SST anomalies with comparable values and durations of wind forcing, shows also a net predominance of ocean processes over air-sea fluxes in generating SST anomalies. Note also its anti-symetrical structure, that reflects the damping effect of latent heat flux that depends strongly upon SST. However, the absence of a closed heat budget prevents a full quantification of the relative contributions of surface heat fluxes and ocean dynamics.

At Cap Blanc, upwelling remains partially active prior to MHW onset, as indicated by a slightly positive Coastal Upwelling Index (CUI; Fig. 7e), suggesting a persistent but weakened dynamical balance between wind forcing and coastal circulation. As a result, thermal preconditioning remains moderate (+0.4–0.5 °C). In contrast, in the southern regime (Grande Côte and Petite Côte), the reduction in wind stress triggers a rapid breakdown of the upwelling circulation, with strongly negative CUI

https://doi.org/10.5194/egusphere-2026-2571
Preprint. Discussion started: 21 May 2026

anomalies (-0.35 to -0.45 °C), indicating a collapse of cold water supply to the surface layer. This dynamical shutdown is accompanied by stronger thermal preconditioning (+0.7–0.8 °C), consistent with heat accumulation in a stratifying upper ocean when advective and vertical cooling are suppressed.

The decay phase further reinforces this mechanistic dichotomy. At Cap Blanc, rapid dissipation of SST anomalies (0.2 °C by J+30) is driven by the rapid re-establishment of latent heat loss (strongly negative anomalies, down to -18 $W\,m^{-2}$), reflecting the restoration of wind-driven evaporative cooling and the reactivation of turbulent heat exchange. This indicates a highly responsive system in which atmospheric forcing rapidly re-establishes thermal equilibrium. By contrast, in the southern regime, recovery is significantly slower, with persistent positive SST anomalies (0.6–0.8 °C at J+30). This delayed recovery reflects the inertia of the stratified upper ocean and the slow re-establishment of seasonal upwelling circulation, once the dynamical suppression has been established. In this context, MHW persistence is governed less by surface flux recovery than by the time scale required to restore vertical and coastal circulation pathways.

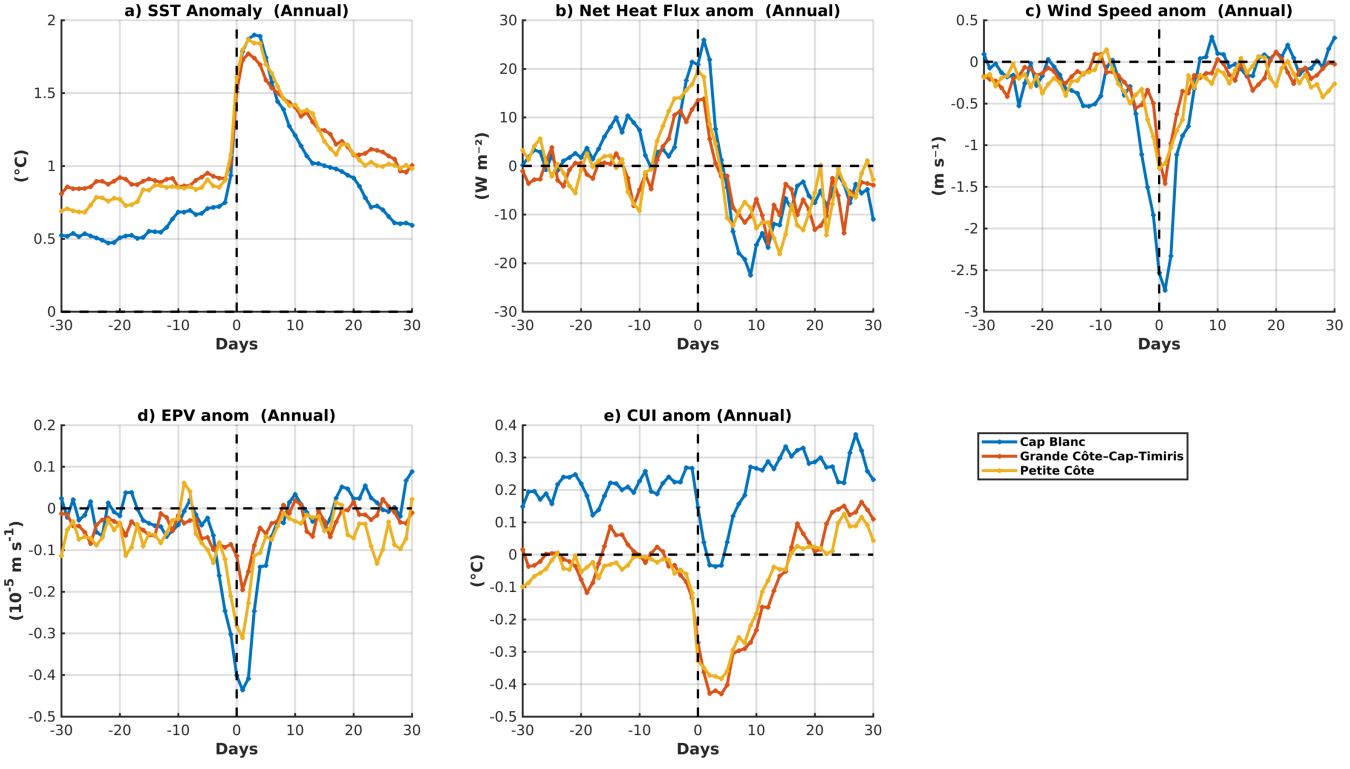

Figure 7. Composite analysis of anomalies in key atmospheric and oceanic forcings surrounding MHWs in the SMUS. (a) SST (°C), (b) net heat flux (W m^{-2}), (c) wind speed (m s^{-1}), (d) Ekman pumping velocity (EPV*10^{-6} m s^{-1}), and (e) Coastal Upwelling Index (CUI) anomalies (°C), for 30 days before and after MHW events. Day 0 corresponds to the onset of MHW events.

https://doi.org/10.5194/egusphere-2026-2571
Preprint. Discussion started: 21 May 2026

3.3.2 Seasonal modulation: comparison between CP and WP

The two-period (CP and WP) partition of the MHW composite is presented (Fig. 8). As seen in Section 3.1.2, the amplitude hierarchy of SST signals depends on the period, with MHW intensity increasing southward from 1.7 to 2.1°C during CP, and northward from 1.4 to 2.1°C during WP, following the meridional migration of the upwelling front. The wind stress forcing, by contrast, is weakly dependent on the period in the central and northern regions and displays, at first order, a quasi-symmetrical relaxation signal relative to time zero of the MHW composite, especially when neglecting frequencies higher than 10 days. In the Petite Côte, wind relaxation exhibits a significantly weaker amplitude during the warm WP, which is accompanied by a reduced Ekman pumping response.

Regarding the response of CUI to MHWs, a clear seasonal and regional dependency emerges across the SMUS sub-coastal regions. In the permanent upwelling region of Cap Blanc, CUI remains weakly negative during the CP (CUI < -0.2 °C; Fig. 8e1), indicating that upwelling persists but is insufficient to counterbalance surface warming. In contrast, during the WP, coastal upwelling is strongly weakened (CUI < -0.4 °C). This seasonal structuring is partially masked in annual composites, which smooth CP/WP contrasts and therefore underestimate the true seasonal modulation of the upwelling response. This regime shift implies a strong reduction in nutrient supply to the euphotic zone, with direct implications for primary productivity, which are further discussed in Section 3.4. In the seasonal upwelling region, particularly in its southernmost part (Petite Côte), the upwelling response is negative and more pronounced during the CP (approximately -0.5 °C) than during the WP (approximately -0.2 °C). In the intermediate region (Grande Côte), the response is also negative and remains stronger during the CP (approximately -0.5 °C) than during the WP (approximately -0.4 °C), although the seasonal contrast is weaker there.

To understand better, it is important to realize that, following Faye et al. (2015), the advective and turbulent heat fluxes of ocean dynamics, associated to the presence of the upwelling meridional front, are maximal during CP. The analysis of Fig. 8b1 and Fig. 8b2 further highlights, in addition to this seasonal contrast, a strong latitudinal dependency. At Cap Blanc, in the northern SMUS, net surface heat flux anomalies reach particularly high values (+35 to +40 W m^{-2}), compared to much lower values during the WP (below 20 W m^{-2}). In contrast, in the southern regions (Grande Côte and Petite Côte), values are slightly higher during the CP.

The seasonal comparison between permanent and seasonal upwelling zones reveals a clear mechanistic opposition. During the CP, Cap Blanc is characterized by a strong air–sea coupling, with high net heat fluxes (+35 to +40 W m^{-2}) and a relatively weak upwelling response (CUI ≈ -0.20), reflecting a dynamical system capable of partially sustaining upwelling despite intense atmospheric forcing. In contrast, southern regions exhibit a stronger CUI response (-0.45 to -0.50), indicating a higher sensitivity of the upwelling circulation to wind forcing and a more efficient destabilization of the thermal structure. During the WP, Cap Blanc tends to converge toward southern regimes in terms of surface heat flux, yet maintains a faster dissipation of SST anomalies, highlighting the dominant role of local dynamics in controlling MHW persistence. Notably, wind anomalies at Cap Blanc are systematically the strongest (≈ -3.0 m s^{-1}) regardless of season, yet paradoxically generate the least persistent MHWs events, underscoring that the vulnerability of local upwelling dynamics, rather than the intensity of atmospheric forcing, ultimately governs the severity and persistence of these events.

https://doi.org/10.5194/egusphere-2026-2571
Preprint. Discussion started: 21 May 2026

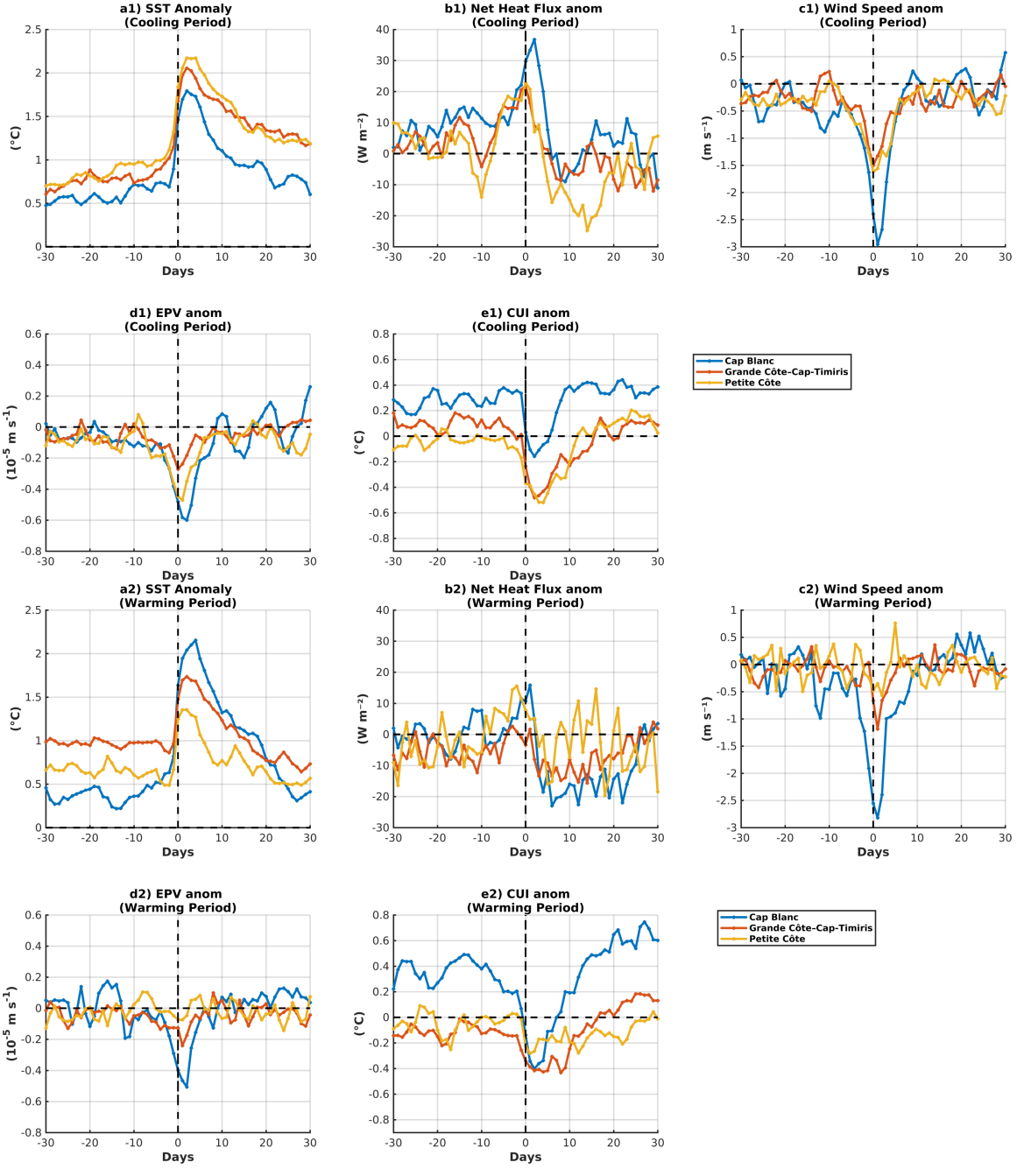

Figure 8. Composite analysis of anomalies in key atmospheric and oceanic forcings surrounding MHWs by season. The left panels (a1–e1) represent the cooling period (November–May), and the right panels (a2–e2) represent the warming period (June–October). (a) SST (°C), (b) net heat flux (Qnet, W m^{-2}), (c) 10 m wind speed (m s^{-1}), (d) Ekman pumping velocity (EPV*10^{-6} m s^{-1}), and (e) Coastal Upwelling Index (CUI, °C). Lines indicate composites for Cap Blanc (blue), Grande Côte (red), and Petite Côte (orange). Day 0 (dashed vertical line) corresponds to the onset of MHW events. The composites include 158 events for the cooling period and 125 events for the warming period over the period 1982–2024.

https://doi.org/10.5194/egusphere-2026-2571
Preprint. Discussion started: 21 May 2026

3.4 Phytoplankton biomass response to MHWs

Temporal composites (±30-day window around MHW onset) and spatial composites (averaged over each event) of chlorophyll-a anomalies highlight a pronounced asymmetry in phytoplankton responses (Noh et al., 2022) between the permanent upwelling region of Cap Blanc and the southern seasonal upwelling regions of the SMUS (Grande Côte and Petite Côte).

The magnitude of biomass decline is strongly seasonally modulated. During the CP, chlorophyll-a anomalies reach -2 mg m^{-3} (Grande Côte) and -1.5 mg m^{-3} (Petite Côte), compared with weaker reductions (-0.3 to -0.5 mg m^{-3}) during the WP (Figs. 9b1-c1). This seasonal contrast reflects differences in the background state of the ecosystem: during the CP, the system is typically nutrient-replete due to climatological upwelling, such that MHW-induced suppression of upwelling produces a strong negative nutrient anomaly relative to baseline conditions. Spatial composites confirm a coherent coastal band of strongly negative anomalies (down to -2.4 mg m^{-3}) extending offshore (14–18°N ; Fig. 9b2), consistent with basin-scale suppression of nutrient-driven primary production under peak thermal stress.

In these southern coastal upwelling regions (Grande Côte and Petite Côte), phytoplankton responses emerge early and persist throughout the MHW lifecycle and is consistent with a nutrient-limited regime triggered by dynamical upwelling collapse. Temporally, chlorophyll-a anomalies become negative as early as J-30 (Fig. 9a1) and progressively intensify, reaching their minimum during and shortly after MHW onset (J0 to J+15). This indicates a sustained decline in phytoplankton biomass. This early response likely reflects ecosystem sensitivity to wind relaxation, reduced Ekman transport which progressively weakens the upward flux of nutrients into the euphotic zone , and the progressive accumulation of positive thermal anomalies preceding MHW detection. Thus, within the N–L–T framework, this regime is primarily controlled by the nutrient term, as coastal upwelling collapse (CUI < $-0.4\,^{\circ}$C; Fig. 8e1) strongly reduces nitrate injection into the surface layer. Although temperature increases during MHWs may enhance phytoplankton metabolic rates (T-effect), this positive physiological response is overwhelmed by nutrient limitation. Light availability plays a secondary but reinforcing role through increased stratification, which further restricts vertical nutrient renewal.

In contrast, the northern SMUS (Cap Blanc) exhibits a fundamentally different and seasonally reversed phytoplankton response, consistent with the dynamical regimes described in Section 3.3.2. During the CP, chlorophyll-a anomalies become positive early in the MHW lifecycle (as early as J-15), peaking between J0 and J+5 at approximately +2.3 mg m^{-3} (Fig. 9b1). This pattern is further supported by event-scale statistics: 64.7% of MHW events during the CP are associated with a positive chlorophyll-*a* response, compared to only 23.1% during the WP (Table 3). This positive response likely reflects the interaction between residual upwelling-driven nutrient supply and MHW-related surface warming. In this regime, the nutrient term does not collapse because upwelling persists in a weakened but non-zero state (CUI > +0.4 °C during preconditioning, slightly negative during MHW onset; Fig. 8e1). Consequently, nutrient limitation is alleviated relative to the southern regime. Simultaneously, the temperature term exerts a positive control by enhancing metabolic rates, photosynthetic efficiency, and growth kinetics, particularly under non-limiting nutrient conditions (Marañón et al., 2018). The light term may also contribute positively through increased surface stratification, which can enhance light exposure within the mixed layer and improve photosynthetic conditions (Noh et al., 2022). The resulting response is therefore best interpreted as a co-limitation release

https://doi.org/10.5194/egusphere-2026-2571
Preprint. Discussion started: 21 May 2026

regime, where moderate warming enhances biological activity under residual nutrient availability (Hayashida et al., 2020). This interpretation is consistent with experimental evidence showing that moderate warming can enhance phytoplankton biomass production and accelerate bloom dynamics when nutrients are not strongly limiting (López-Sandoval et al., 2025).

This mechanistic interpretation is further supported by contrasting conditions during the WP. During the WP at Cap Blanc, however, this balance shifts toward a nutrient-limited stratified regime. Stronger MHW intensities (>2 °C) coincide with negative chlorophyll anomalies (Fig. 9c1), indicating a transition to nutrient control dominance. In this case, enhanced thermal stratification, the absence of persistent upwelling, and the influence of large-scale circulation patterns (Lathuiliere et al., 2008; Faye et al., 2015), likely suppress vertical mixing and strongly limit nutrient supply to the euphotic zone, resulting in reduced phytoplankton biomass. Here, enhanced stratification suppresses vertical mixing, effectively decoupling the euphotic zone from deeper nutrient reservoirs. The nutrient term becomes strongly negative, while any positive temperature effect is offset by resource limitation. This results in reduced phytoplankton biomass despite favorable thermal conditions.

Spatial composites further reinforce this seasonal regime shift. During the CP (Fig. 9b2), positive chlorophyll anomalies (up to +3.0 mg m^{-3}) are observed along the Cap Blanc coastal margin, consistent with a nutrient-replete, mixed-control regime (N + T co-activation) sustained by residual upwelling. In contrast, during the WP (Fig. 9c2), the same region exhibits strong negative chlorophyll anomalies (-1.8 to -2.4 mg m^{-3}), indicating strong thermal regime and reflecting a transition to a stratification-driven nutrient limitation regime, spatially aligned with maximum MHW intensity and driving the suppression of chlorophyll biomass production. Wind vector anomalies superimposed on spatial composites provide a consistent dynamical interpretation of the mechanisms described in 3.3.2. At the annual scale and during the cooling period (Fig. 9a2-b2), wind anomalies exhibit a southwesterly orientation, opposite to the climatological northeasterly trade winds that favor upwelling. This reversal indicates a generalized relaxation of trade winds during MHW events, consistent with a reduction in Ekman transport and coastal upwelling intensity.

Overall, in contrast to temperate EBUS where MHWs generally tend to reduce phytoplankton biomass through the weakening of upwelling and the associated decline in nutrient supply (Li et al., 2024; Zhan et al., 2024), phytoplankton responses in the SMUS exhibit marked heterogeneity in chlorophyll-a, reflecting a strong regional asymmetry between the southern seasonal upwelling regions (Grande Côte and Petite Côte) and the northern permanent upwelling system (Cap Blanc).

https://doi.org/10.5194/egusphere-2026-2571
Preprint. Discussion started: 21 May 2026

Table 3. Proportion of MHW events associated with a positive chlorophyll-a anomaly (mean anomaly > 0 integrated over the full event duration) in the three SMUS sub-regions over the period 1998–2024, for the annual, cooling (November–May), and warming (June–October) periods. Values indicate the number of positive-response events over the total number of detected events, with the corresponding percentage in parentheses. For the southern upwelling regions (Grande Côte and Petite Côte), only the cooling period results are physically interpretable within the upwelling framework (see Section 3.4).

Sub-region	Annual	Cooling (Nov–May)	Warming (Jun–Oct)
Cap Blanc	28/60 (46.7%)	22/34 (64.7%)	6/26 (23.1%)
Grande Côte	7/50 (14.0%)	3/29 (10.3%)	4/21 (19.0%)*
Petite Côte	15/50 (30.0%)	9/34 (26.5%)	6/16 (37.5%)*

* Not physically interpretable within the upwelling framework (see text).

https://doi.org/10.5194/egusphere-2026-2571
Preprint. Discussion started: 21 May 2026

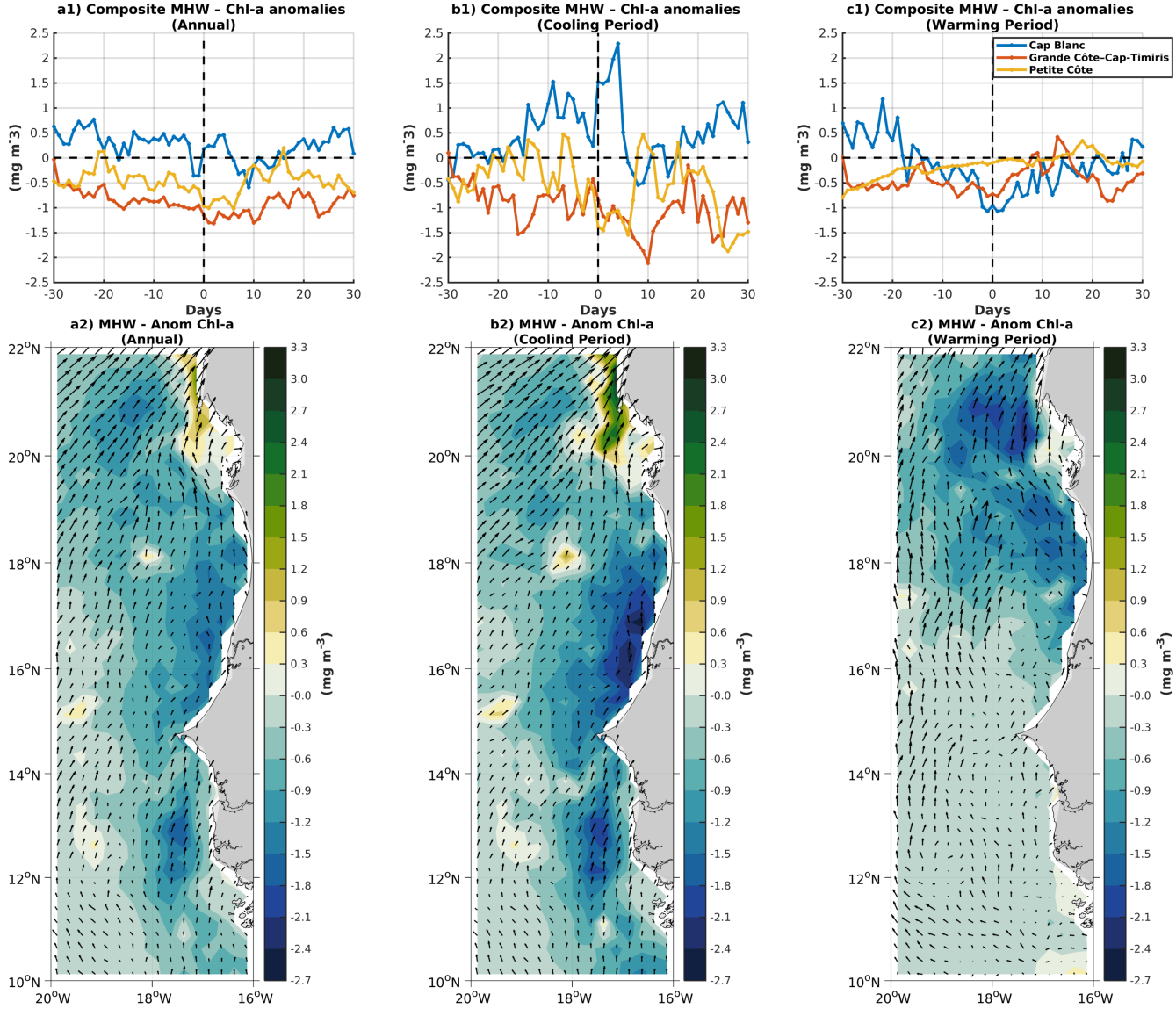

Figure 9. Chlorophyll-a response to MHWs in the SMUS (1998–2024). Top row (a1–c1): temporal composites of chlorophyll-a anomalies over a ±30-day window around MHW onset for Cap Blanc (blue), Grande Côte (orange), and Petite Côte (yellow). Day 0 corresponds to the event onset. Bottom row (a2–c2): spatial composites of chlorophyll-a anomalies (mg m^{-3}, color shading) overlaid with 10 m wind vector anomalies, computed over the full event duration (start to end). Columns correspond, respectively, to the annual analysis, the cooling period, and the warming period.

https://doi.org/10.5194/egusphere-2026-2571
Preprint. Discussion started: 21 May 2026

4 Conclusion

This study provides a comprehensive analysis of the spatio-temporal characteristics, long-term trends, and local physical processes of marine heatwaves (MHWs), as well as their relationship with phytoplankton biomass in the Senegal–Mauritania Upwelling System (SMUS) over the period 1982–2024, based on high-resolution satellite data and reanalysis products. MHWs in the SMUS result from a complex interaction between global ocean warming, regional atmospheric forcing, and the seasonal dynamics of coastal upwelling, with major consequences for phytoplankton biomass and marine ecosystems. In eastern boundary upwelling systems, upwelling generally acts as a thermal buffer by supplying cold, nutrient-rich waters, but in the SMUS this buffering capacity is modulated by its tropical seasonality, with peak upwelling occurring during the cooling period (November–May). Although this should limit extreme warming events, the system remains highly sensitive to wind variability and large-scale climate modes, while also sustaining high biological productivity that underpins a key socio-economic fishery.

Between 1982 and 2024, MHWs exhibit strong spatial, seasonal, and temporal variability. Offshore and weak-upwelling regions (e.g., Banc d'Arguin, Bijagós, and the open ocean) experience the highest frequency and duration of MHWs due to stronger surface warming and weaker vertical mixing. In contrast, persistent upwelling zones such as Cap Blanc and the Petite Côte act as thermal refugia, with fewer and shorter events, although they may still experience high-intensity anomalies associated with strong coastal thermal gradients. Seasonally, MHWs are more frequent and longer during the cooling period, when upwelling is typically strongest, indicating that short-term disruptions of upwelling during this season have particularly strong effects. Over the long term, MHW frequency and duration have increased significantly, especially since the mid-1990s, under the combined influence of anthropogenic warming and climate variability (e.g., the Atlantic Multidecadal Oscillation and El Niño).

Physically, MHWs are consistently triggered by a weakening of trade winds, which reduces Ekman transport and suppresses upwelling. However, the oceanic response varies across regions and seasons. In the northern SMUS, characterized by a quasi-permanent upwelling regime (Cap Blanc), upwelling remains partially active even during wind relaxation, leading to moderate heat accumulation and a rapid, thermodynamically driven MHW response. In contrast, in the southern regions, associated with seasonal upwelling (Grande Côte and Petite Côte), wind relaxation leads to a near-complete collapse of upwelling, suppressing both cooling and nutrient supply. This results in stronger and more persistent heat accumulation, with slower development but longer-lasting MHWs. This defines a clear dichotomy between a northern regime dominated by thermodynamics and rapid adjustment, and a southern regime controlled by dynamics and more persistent.

These physical differences translate directly into contrasting biological responses. In the southern seasonal upwelling regions, MHWs lead to a strong decline in chlorophyll-a due to reduced nutrient supply to the euphotic zone. This results in a nutrient-limited regime, in which chlorophyll anomalies become negative early and intensify throughout the event, particularly during the cooling period when baseline productivity is typically high. In this context, nutrient limitation dominates over any potential positive temperature effects on phytoplankton metabolism, leading to substantial reductions in primary productivity. Spatially, this appears as a broad coastal band of negative chlorophyll anomalies extending offshore.

https://doi.org/10.5194/egusphere-2026-2571
Preprint. Discussion started: 21 May 2026

In contrast, the permanent upwelling system at Cap Blanc exhibits a more complex and seasonally dependent response. During the cooling period, the partial persistence of upwelling supports a mixed nutrient–temperature regime, in which moderate warming enhances phytoplankton growth, resulting in positive chlorophyll anomalies. During the warming period, however, stronger stratification and weaker upwelling lead to nutrient limitation and negative anomalies, particularly during high-intensity events. Wind anomalies associated with the weakening or reversal of trade winds provide the physical link between atmospheric forcing, upwelling suppression, and ecosystem response.

Overall, the SMUS illustrates that MHWs are not purely thermal phenomena but coupled physical–biological events. While global warming drives their increasing frequency and duration, their ecological impacts are primarily controlled by changes in upwelling dynamics. Where upwelling collapses, MHWs lead to strong reductions in phytoplankton biomass; where it persists, they may temporarily enhance productivity under certain conditions. This dual behavior highlights the combined importance of atmospheric forcing and ocean dynamics in regulating ecosystem responses. Finally, this study emphasizes the vulnerability of this highly productive system, where disruptions to the balance between temperature, nutrients, and circulation can have significant ecological and socio-economic consequences, particularly for fisheries.

Data availability.

All datasets used in this study are publicly available from open-access repositories. The sea surface temperature (SST) data were obtained from the NOAA Optimum Interpolation Sea Surface Temperature dataset (OISST, version 2.1), available at https://www.ncei.noaa.gov/data/sea-surface-temperature-optimum-interpolation/v2.1/access/avhrr/ (accessed on 10 October 2025). Atmospheric variables (10 m wind components, surface heat fluxes) were extracted from the ECMWF ERA5 reanalysis, distributed via the Copernicus Climate Data Store at https://cds.climate.copernicus.eu/cdsapp#!/dataset/reanalysis-era5-single-levels (accessed on 10 October 2025). Chlorophyll-*a* concentration data were obtained from the Copernicus Marine Environment Monitoring Service (CMEMS), available at https://marine.copernicus.eu/ (accessed on October 2025), under CMEMS terms and conditions. All datasets are freely accessible from the links provided above. No proprietary or restricted data were used in this study.

Code and data availability. Marine heatwave detection and characterization were performed using the marineHeatWaves toolbox (Zhao and Marin, 2019), available at https://github.com/ZijieZhaoMMHW/m_mhw1.0/blob/master/. The code was used without modification. A reproducible workflow is ensured through open-source implementation.

Author contribution. Waly Dione: conceptualization, methodology, formal analysis, writing – original draft, visualization, figure production. Ibrahima Camara: review and editing. Alban Lazar: supervision, methodology, review and editing. Diana Ruiz-Pino: supervision, review and editing. Amadou Thierno Gaye: doctoral supervision and scientific oversight.

Competing interests. The authors declare that they have no conflict of interest.

https://doi.org/10.5194/egusphere-2026-2571
Preprint. Discussion started: 21 May 2026

References

Abrahams, A., Schlegel, R. W., and Smit, A. J.: Variation and change of upwelling dynamics detected in the world's eastern boundary upwelling systems, Frontiers in Marine Science, 8, 626 411, 2021.

Arístegui, J., Barton, E. D., Álvarez-Salgado, X. A., Santos, A. M. P., Figueiras, F. G., Kifani, S., Hernández-León, S., Mason, E., Machú, E., and Demarcq, H.: Sub-regional ecosystem variability in the Canary Current upwelling, Progress in Oceanography, 83, 33–48, 2009.

Bakun, A.: Coastal upwelling indices, west coast of North America, 1946-71, 1973.

Bakun, A., Black, B. A., Bograd, S. J., Garcia-Reyes, M., Miller, A. J., Rykaczewski, R. R., and Sydeman, W. J.: Anticipated effects of climate change on coastal upwelling ecosystems, Current Climate Change Reports, 1, 85–93, 2015.

Behr, L., Xoplaki, E., Luther, N., Josey, S. A., and Luterbacher, J.: Atmospheric patterns drive marine heatwaves in the North Atlantic and Mediterranean Sea during summer 2023, Environmental Research Letters, 20, 104 020, 2025.

Benazzouz, A., Mordane, S., Orbi, A., Chagdali, M., Hilmi, K., Atillah, A., Pelegrí, J. L., and Hervé, D.: An improved coastal upwelling index from sea surface temperature using satellite-based approach–The case of the Canary Current upwelling system, Continental Shelf Research, 81, 38–54, 2014.

Black, I. T., Kavanaugh, M. T., and Reimers, C. E.: Bloom compression alongside marine heatwaves contemporary with the Oregon upwelling season, Limnology and Oceanography, 70, S136–S149, 2025.

Boely, T., Chabanne, J., Fréon, P., and Stequert, B.: Cycle sexuel et migrations de Sardinella aurita sur le plateau ouest-africain des iles Bissagos a la Mauritanie, in: Symp. sur le courant des Canaries: upwelling et resources vivantes. Las Palmas, 92, pp. 1–12, 1978.

Chabert, P., Capet, X., Echevin, V., Lazar, A., Hourdin, C., and Ndoye, S.: Impact of synoptic wind intensification and relaxation on the dynamics and heat budget of the south Senegalese upwelling sector, Journal of Physical Oceanography, 53, 1041–1067, 2023.

Chavez, F. P. and Messié, M.: A comparison of eastern boundary upwelling ecosystems, Progress in Oceanography, 83, 80–96, 2009.

Cropper, T. E., Hanna, E., and Bigg, G. R.: Spatial and temporal seasonal trends in coastal upwelling off Northwest Africa, 1981–2012, Deep Sea Research Part I: Oceanographic Research Papers, 86, 94–111, 2014.

DeCastro, M., Gómez-Gesteira, M., Costoya, X., and Santos, F.: Upwelling influence on the number of extreme hot SST days along the Canary upwelling ecosystem, Journal of Geophysical Research: Oceans, 119, 3029–3040, 2014.

Demarcq, H.: Trends in primary production, sea surface temperature and wind in upwelling systems (1998–2007), Progress in Oceanography, 83, 376–385, 2009.

Deme, M., Failler, P., et al.: Small pelagic fish in Senegal: a multi-usage resource, Marine Policy, 141, 105 083, 2022.

Diakhaté, M., De Coëtlogon, G., Lazar, A., Wade, M., and Gaye, A. T.: Intraseasonal variability of tropical Atlantic sea-surface temperature: air–sea interaction over upwelling fronts, Quarterly Journal of the Royal Meteorological Society, 142, 372–386, 2016.

Durant, J., Molinero, J., Ottersen, G., Reygondeau, G., Stige, L., and Langangen, Ø.: Contrasting effects of rising temperatures on trophic interactions in marine ecosystems. Sci Rep 9: 15213, 2019.

Ekman, V. W.: On the influence of the earth's rotation on ocean-currents, Arkiv för Matematik, Astronomi och Fysik, 2, 1–53, 1905.

Enfield, D. B., Mestas-Nuñez, A. M., and Trimble, P. J.: The Atlantic multidecadal oscillation and its relation to rainfall and river flows in the continental US, Geophysical research letters, 28, 2077–2080, 2001.

Faye, S., Lazar, A., Sow, B. A., and Gaye, A. T.: A model study of the seasonality of sea surface temperature and circulation in the Atlantic North-eastern Tropical Upwelling System, Frontiers in Physics, 3, 76, 2015.

Frölicher, T. L. and Laufkötter, C.: Emerging risks from marine heat waves, Nature communications, 9, 650, 2018.

https://doi.org/10.5194/egusphere-2026-2571
Preprint. Discussion started: 21 May 2026

García-Reyes, M., Koval, G., Sydeman, W. J., Palacios, D., Bedriñana-Romano, L., DeForest, K., Montenegro Silva, C., Sepulveda, M., and Hines, E.: Most eastern boundary upwelling regions represent thermal refugia in the age of climate change, Frontiers in Marine Science, 10, 1158 472, 2023.

Garnesson, P., Mangin, A., Fanton d'Andon, O., Demaria, J., and Bretagnon, M.: The CMEMS GlobColour chlorophyll a product based on satellite observation: multi-sensor merging and flagging strategies, Ocean Science, 15, 819–830, 2019.

Guibourd de Luzinais, V., Cheung, W. W., and Gascuel, D.: Marine heatwaves deeply alter marine food web structure and function, Biogeosciences, 22, 6583–6606, 2025.

Hayashida, H., Matear, R. J., and Strutton, P. G.: Background nutrient concentration determines phytoplankton bloom response to marine heatwaves, Global change biology, 26, 4800–4811, 2020.

Hersbach, H., Bell, B., Berrisford, P., Hirahara, S., Horányi, A., Muñoz-Sabater, J., Nicolas, J., Peubey, C., Radu, R., Schepers, D., et al.: The ERA5 global reanalysis, Quarterly journal of the royal meteorological society, 146, 1999–2049, 2020.

Hobday, A. J., Alexander, L. V., Perkins, S. E., Smale, D. A., Straub, S. C., Oliver, E. C., Benthuysen, J. A., Burrows, M. T., Donat, M. G., Feng, M., et al.: A hierarchical approach to defining marine heatwaves, Progress in oceanography, 141, 227–238, 2016.

Holbrook, N. J., Scannell, H. A., Sen Gupta, A., Benthuysen, J. A., Feng, M., Oliver, E. C., Alexander, L. V., Burrows, M. T., Donat, M. G., Hobday, A. J., et al.: A global assessment of marine heatwaves and their drivers, Nature Communications, 10, 1–13, 2019.

Imbol Koungue, R. A., Prigent, A., Lübbecke, J. F., Brandt, P., and Jouanno, J.: Interannual variability of net primary productivity in the northwest African coastal upwelling system and their relation to Dakar Niños, Scientific reports, 15, 43 875, 2025.

Jacox, M. G., Alexander, M. A., Bograd, S. J., and Scott, J. D.: Thermal displacement by marine heatwaves, Nature, 584, 82–86, 2020.

Kahru, M., Kudela, R. M., Anderson, C. R., Manzano-Sarabia, M., and Mitchell, B. G.: Evaluation of satellite retrievals of ocean chlorophyll-a in the California Current, Remote Sensing, 6, 8524–8540, 2014.

Kendall, M. G.: Rank Correlation Methods, Charles Griffin, London, 4th edn., 1975.

Knight, J. R., Allan, R. J., Folland, C. K., Vellinga, M., and Mann, M. E.: A signature of persistent natural thermohaline circulation cycles in observed climate, Geophysical Research Letters, 32, 2005.

Koné, M., Kouadio, Y. K., and Adon, M.: Relationship Between Tropical Atlantic Marine Heatwaves and Rainfall in West Africa During the Monsoon Period, Advances in Meteorology, 2025, 7899 901, 2025.

Lakhnigue, A., Tandstad, M., Fuller, J., Sambe, B., and Caramelo, A. M.: More than fifteen years of collaboration on the assessment of small pelagic fish off Northwest Africa: Lessons learned and future perspectives, Deep Sea Research Part II: Topical Studies in Oceanography, 159, 92–102, 2019.

Large, W. G. and Pond, S.: Open ocean momentum flux measurements in moderate to strong winds, Journal of physical oceanography, 11, 324–336, 1981.

Lathuiliere, C., Echevin, V., and Lévy, M.: Seasonal and intraseasonal surface chlorophyll-a variability along the northwest African coast, Journal of Geophysical Research: Oceans, 113, 2008.

Li, M., Organelli, E., Serva, F., Bellacicco, M., Landolfi, A., Pisano, A., Marullo, S., Shen, F., Mignot, A., van Gennip, S., et al.: Phytoplankton spring bloom inhibited by marine heatwaves in the North-Western Mediterranean Sea, Geophysical Research Letters, 51, e2024GL109 141, 2024.

López-Sandoval, D. C., Fernández-González, C., González-García, C., and Marañón, E.: Warming Accelerates Phytoplankton Bloom Dynamics and Differentially Affects the Fluxes of Carbon, Nitrogen, and Oxygen Through a Coastal Microbial Community, Microbial Ecology, 88, 117, 2025.

https://doi.org/10.5194/egusphere-2026-2571
Preprint. Discussion started: 21 May 2026

Mann, H. B.: Nonparametric tests against trend, Econometrica: Journal of the econometric society, pp. 245–259, 1945.

Marañón, E., Lorenzo, M. P., Cermeño, P., and Mouriño-Carballido, B.: Nutrient limitation suppresses the temperature dependence of phytoplankton metabolic rates, The ISME journal, 12, 1836–1845, 2018.

Maritorena, S. and Siegel, D. A.: Consistent merging of satellite ocean color data sets using a bio-optical model, Remote Sensing of Environment, 94, 429–440, 2005.

Messié, M. and Chavez, F. P.: Seasonal regulation of primary production in eastern boundary upwelling systems, Progress in Oceanography, 134, 1–18, 2015.

Ndoye, S., Capet, X., Estrade, P., Sow, B., Dagorne, D., Lazar, A., Gaye, A., and Brehmer, P.: SST patterns and dynamics of the southern Senegal-Gambia upwelling center, Journal of Geophysical Research: Oceans, 119, 8315–8335, 2014.

Ningsih, N. S., Beliyana, E., Kamila, I. H., and Tarya, A.: Long-term characteristics of marine heatwaves (1982–2021) in Indonesian water and their impact on upwelling (case study: Southern Java), Frontiers in Marine Science, 12, 1504 995, 2025.

Noh, K. M., Lim, H.-G., and Kug, J.-S.: Global chlorophyll responses to marine heatwaves in satellite ocean color, Environmental Research Letters, 17, 064 034, 2022.

Oettli, P., Morioka, Y., and Yamagata, T.: A regional climate mode discovered in the North Atlantic: Dakar Niño/Niña, Scientific Reports, 6, 18 782, 2016.

Oliver, E. C., Lago, V., Hobday, A. J., Holbrook, N. J., Ling, S. D., and Mundy, C. N.: Marine heatwaves off eastern Tasmania: Trends, interannual variability, and predictability, Progress in oceanography, 161, 116–130, 2018.

Pauly, D. and Christensen, V.: Primary production required to sustain global fisheries, Nature, 374, 255–257, 1995.

Pickett, M. H. and Paduan, J. D.: Ekman transport and pumping in the California Current based on the US Navy's high-resolution atmospheric model (COAMPS), Journal of Geophysical Research: Oceans, 108, 2003.

Pietri, A., Colas, F., Mogollon, R., Tam, J., and Gutierrez, D.: Marine heatwaves in the Humboldt current system: from 5-day localized warming to year-long El Niños, Scientific Reports, 11, 21 172, 2021.

Reynolds, R. W., Smith, T. M., Liu, C., Chelton, D. B., Casey, K. S., and Schlax, M. G.: Daily high-resolution-blended analyses for sea surface temperature, Journal of climate, 20, 5473–5496, 2007.

Schlegel, R. W., Oliver, E. C., and Chen, K.: Global assessment of marine heatwaves and their drivers from a unified perspective, Journal of Climate, 34, 3165–3181, 2021.

Seabra, R., Varela, R., Santos, A. M., Gómez-Gesteira, M., Meneghesso, C., Wethey, D. S., and Lima, F. P.: Reduced nearshore warming associated with eastern boundary upwelling systems, Frontiers in Marine Science, 6, 104, 2019.

Sen, P. K.: Estimates of the regression coefficient based on Kendall's tau, Journal of the American statistical association, 63, 1379–1389, 1968.

Smale, D. A., Wernberg, T., Oliver, E. C., Thomsen, M., Harvey, B. P., Straub, S. C., Burrows, M. T., Alexander, L. V., Benthuysen, J. A., Donat, M. G., et al.: Marine heatwaves threaten global biodiversity and the provision of ecosystem services, Nature Climate Change, 9, 306–312, 2019.

Smith, K. E., Burrows, M. T., Hobday, A. J., King, N. G., Moore, P. J., Sen Gupta, A., Thomsen, M. S., Wernberg, T., and Smale, D. A.: Biological impacts of marine heatwaves, Annual review of marine science, 15, 119–145, 2023.

Sylla, A., Mignot, J., Capet, X., and Gaye, A. T.: Weakening of the Senegalo–Mauritanian upwelling system under climate change, Climate Dynamics, 53, 4447–4473, 2019.

https://doi.org/10.5194/egusphere-2026-2571
Preprint. Discussion started: 21 May 2026

Sylla, A., Sanchez Gomez, E., Mignot, J., and López-Parages, J.: Impact of increased resolution on the representation of the Canary upwelling system in climate models, Geoscientific Model Development, 15, 8245–8267, 2022.

Varela, R., Rodríguez-Díaz, L., de Castro, M., and Gómez-Gesteira, M.: Influence of Canary upwelling system on coastal marine heatwaves, Scientific Reports, 11, 1–11, 2021.

Vázquez, R., Parras-Berrocal, I. M., Koseki, S., Cabos, W., Sein, D. V., and Izquierdo, A.: Seasonality of coastal upwelling trends in the Mauritania-Senegalese region under RCP8. 5 climate change scenario, Science of The Total Environment, 898, 166 391, 2023.

Wang, S., Jing, Z., Wu, L., Sun, S., Peng, Q., Wang, H., Zhang, Y., and Shi, J.: Southern hemisphere eastern boundary upwelling systems emerging as future marine heatwave hotspots under greenhouse warming, Nature communications, 14, 28, 2023.

Yu, Y., Lin, Z., Liu, N., Ding, R., Hu, L., Zheng, H., Zhang, T., and Li, J.: Classification and mechanisms for different types of marine heatwaves in the western Indian Ocean during the past three decades, Atmospheric and Oceanic Science Letters, p. 100729, 2025.

Zeeberg, J., Corten, A., Tjoe-Awie, P., Coca, J., and Hamady, B.: Climate modulates the effects of Sardinella aurita fisheries off Northwest Africa, Fisheries Research, 89, 65–75, 2008.

Zhan, W., Feng, M., Zhang, Y., Shen, X., Zhan, H., and He, Q.: Reduced and smaller phytoplankton during marine heatwaves in eastern boundary upwelling systems, Communications Earth & Environment, 5, 629, 2024.

Zhao, Z. and Marin, M.: A MATLAB toolbox to detect and analyze marine heatwaves, Journal of Open Source Software, 4, 1124, 2019.

Appendix A

The seasonal cycle of the CUI reveals a tripartite organization of the SMUS, which directly shapes the dynamics of marine heatwaves. In the northern region (Cap Blanc, 20–22°N), the CUI remains positive throughout the year (+1.2 to +2.4°C, (Fig. A1a2), indicating a quasi-permanent upwelling regime that acts as a relative thermal refuge. In the central (Grande Côte, 14–19°N) and southern (Petite Côte, 12–14°N) regions, the CUI is positive from November to May (+1.5 to +2.0°C) and then turns negative from June to October (-0.4 to -0.5°C), reflecting a complete cessation of cold water upwelling and the establishment of downwelling conditions.

This seasonal alternation is consistent with the EPV, which decreases from $+40$–$47 \times 10^{-5}\ \mathrm{m\,s^{-1}}$ in winter to less than $7 \times 10^{-5}\ \mathrm{m\,s^{-1}}$ in summer at the Petite Côte (Fig. A1b2). This marked seasonal variability in coastal cooling constitutes a key mechanism modulating the occurrence, intensity, and seasonality of marine heatwaves in the SMUS, as analyzed in the following sections.

https://doi.org/10.5194/egusphere-2026-2571
Preprint. Discussion started: 21 May 2026

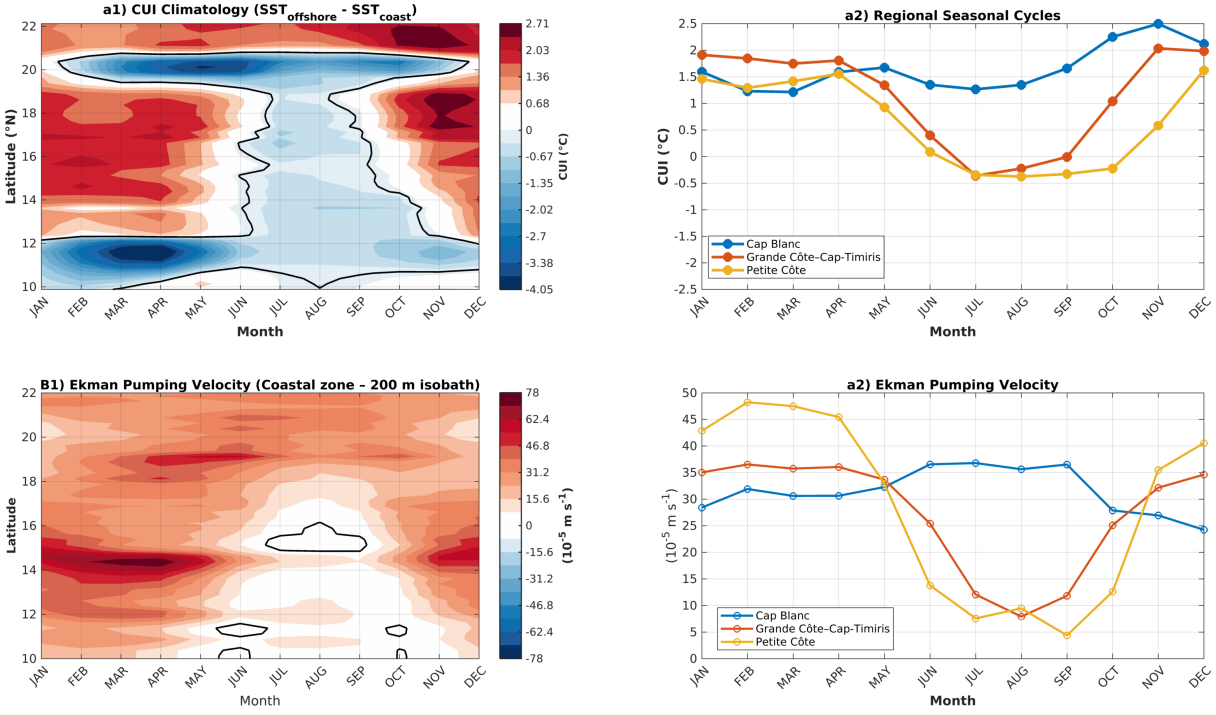

Figure A1. Seasonal variability of upwelling dynamics in the SMUS (1982–2024). a1) Hovmöller diagram (latitude–time) of the climatology of the Coastal Upwelling Index (CUI = $SST_{offshore}$ - SST_{coast}, °C). The black contour marks the zero-CUI line (upwelling/downwelling transition). a2) Regional seasonal cycles of the CUI for the three sub-regions. b1) Hovmöller diagram of the Ekman Pumping Velocity (EPV, 10^{-5} m s^{-1}). Black contours indicate downwelling regions (EPV < 0). b2) Regional seasonal cycles of EPV. The three sub-regions are represented: Cap Blanc (blue), Grande Côte (orange), and Petite Côte (yellow).

https://doi.org/10.5194/egusphere-2026-2571
Preprint. Discussion started: 21 May 2026

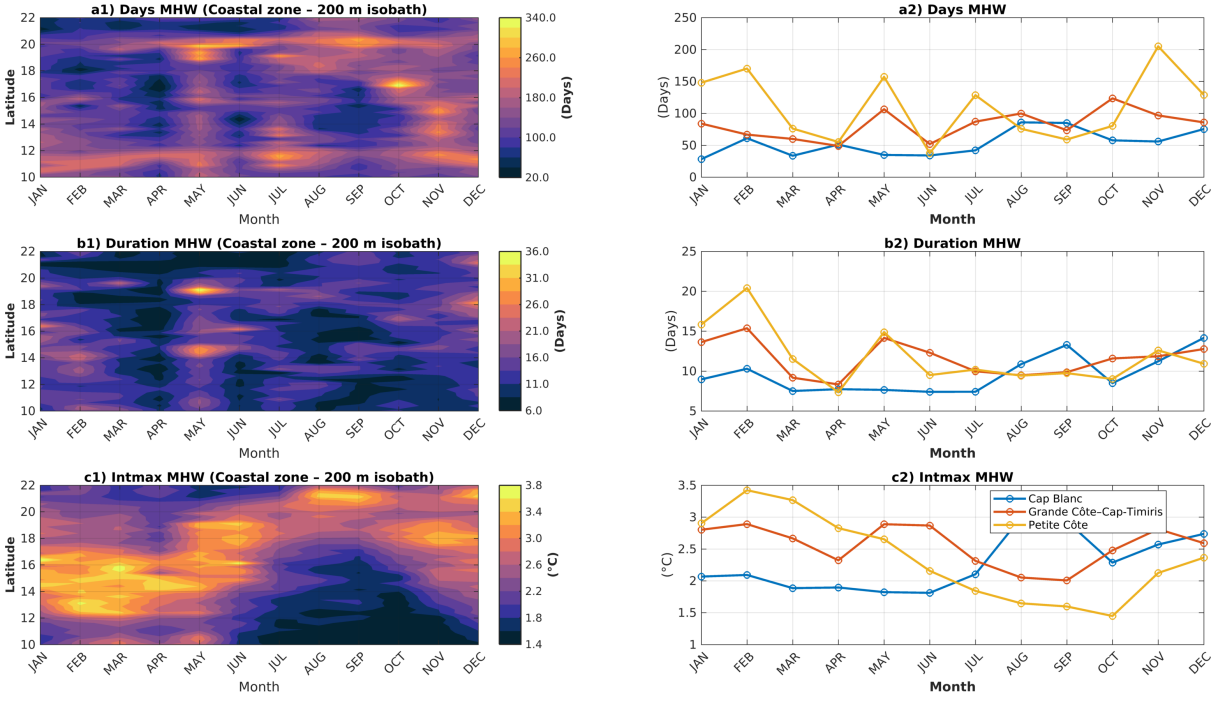

Figure A2. Spatio-temporal variability of marine heatwave (MHW) characteristics over the SMUS coastal shelf. Left panels (a1, b1, c1): Hovmöller diagrams (latitude–time) showing the seasonal and latitudinal distribution (10°N–22°N) of a1 MHW total number of MHW days (number of days per year, 1982–2024), b1 mean duration of MHW events (days), and c1 maximum MHW intensity (°C) along the coastal shelf at the 200 m isobath. Right panels (a2, b2, c2): regional mean seasonal cycles of the same characteristics for three key sub-regions of the continental shelf: Cap Blanc (blue), Grande Côte (orange), and Petite Côte (yellow circles).

https://doi.org/10.5194/egusphere-2026-2571
Preprint. Discussion started: 21 May 2026

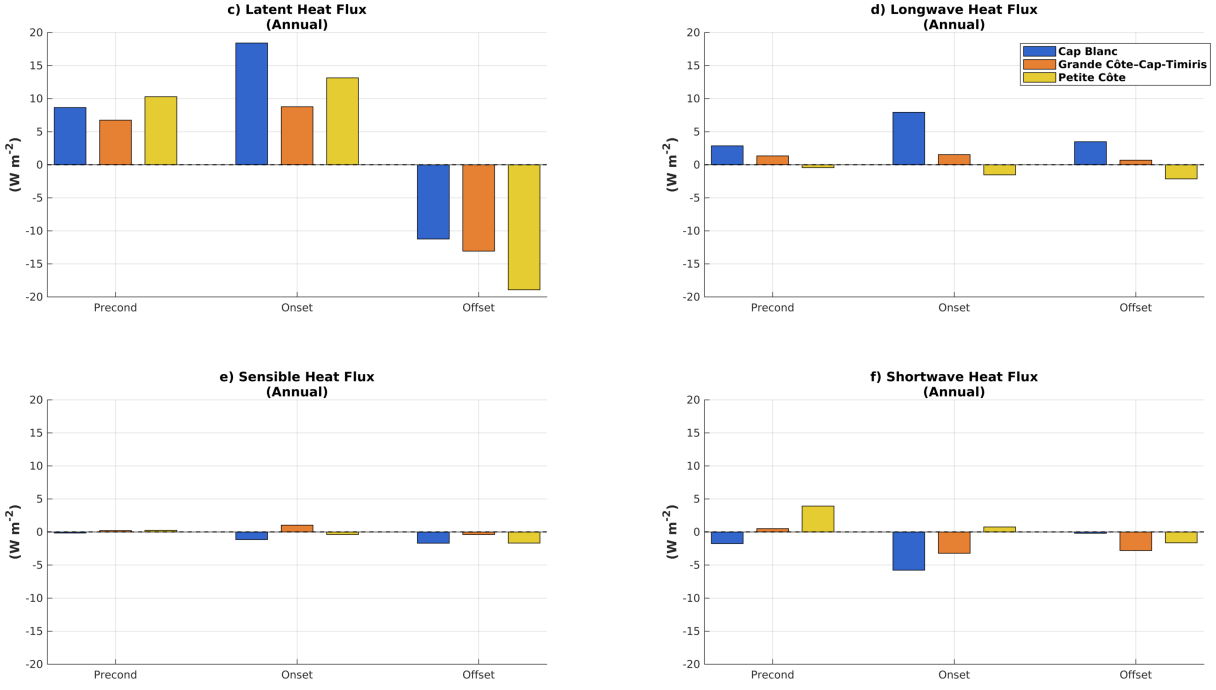

Figure A3. Composites of air-sea heat flux components during marine heatwaves (MHWs) in the three SMUS sub-regions. Panels c–f show the annual anomalies of latent heat flux, longwave heat flux, sensible heat flux, and shortwave heat flux, respectively, for the Precondition, Onset, and Offset phases of MHWs. Positive latent heat flux anomalies during the Onset (+18 W m^{-2} at Cap Blanc; +13 W m^{-2} at Petite Côte) indicate reduced evaporation due to weakened winds, favoring thermal accumulation at the surface. At Offset, the latent heat flux reverses strongly (up to -18 W m^{-2} at Petite Côte), contributing to the gradual dissipation of the thermal anomaly. Incident shortwave radiation shows a notable negative anomaly at Cap Blanc (-5 W m^{-2}) during Onset, consistent with increased cloudiness. Sensible and longwave heat fluxes remain negligible across regions and phases. Cap Blanc (blue), Grande Côte (orange), Petite Côte (yellow).

https://doi.org/10.5194/egusphere-2026-2571
Preprint. Discussion started: 21 May 2026

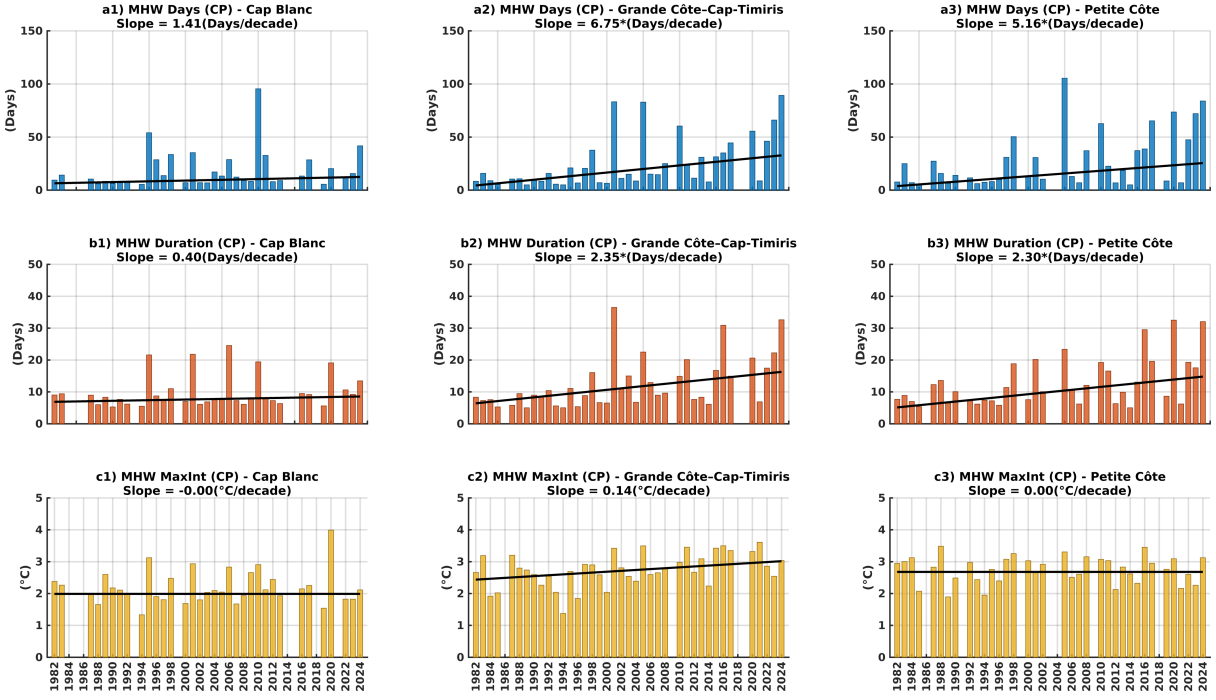

Figure A4. Interannual variability and long-term trends of marine heatwaves (MHWs) in the three SMUS sub-regions during the CP over the 1982–2024 period. Panels a, b, and c represent, respectively: (a) the total annual number of MHW days, (b) the mean event duration (days), and (c) the maximum intensity (°C). Solid lines represent linear trends estimated using Sen's slope method. Reported values indicate the decadal rate of change for each region: Cap Blanc (blue), Grande Côte (orange), and Petite Côte (yellow). The asterisk (*) denotes statistical significance at the 95% confidence level ($p < 0.05$, Mann–Kendall test).

https://doi.org/10.5194/egusphere-2026-2571
Preprint. Discussion started: 21 May 2026

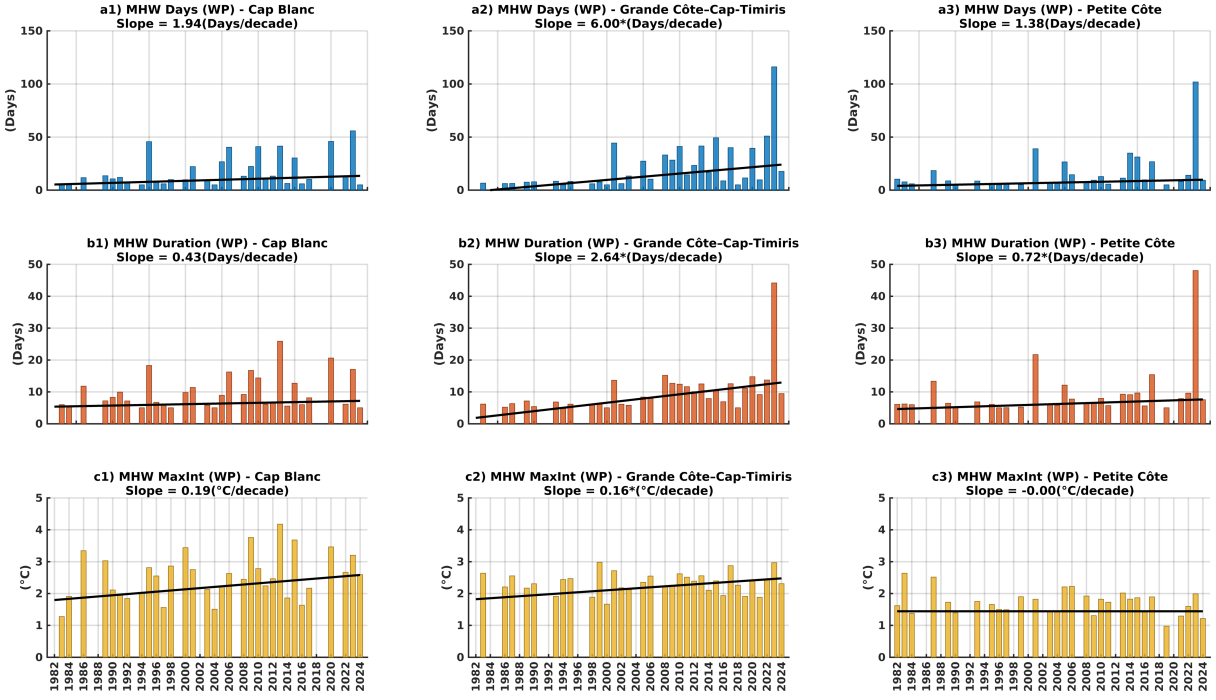

Figure A5. Interannual variability and long-term trends of marine heatwaves (MHWs) in the three SMUS sub-regions during the WP over the 1982–2024 period. Panels a, b, and c represent, respectively: (a) the total annual number of MHW days, (b) the mean event duration (days), and (c) the maximum intensity (°C). Solid lines represent linear trends estimated using Sen's slope method. Reported values indicate the decadal rate of change for each region: Cap Blanc (blue), Grande Côte (orange), and Petite Côte (yellow). The asterisk (*) denotes statistical significance at the 95% confidence level ($p < 0.05$, Mann–Kendall test).

https://doi.org/10.5194/egusphere-2026-2571
Preprint. Discussion started: 21 May 2026

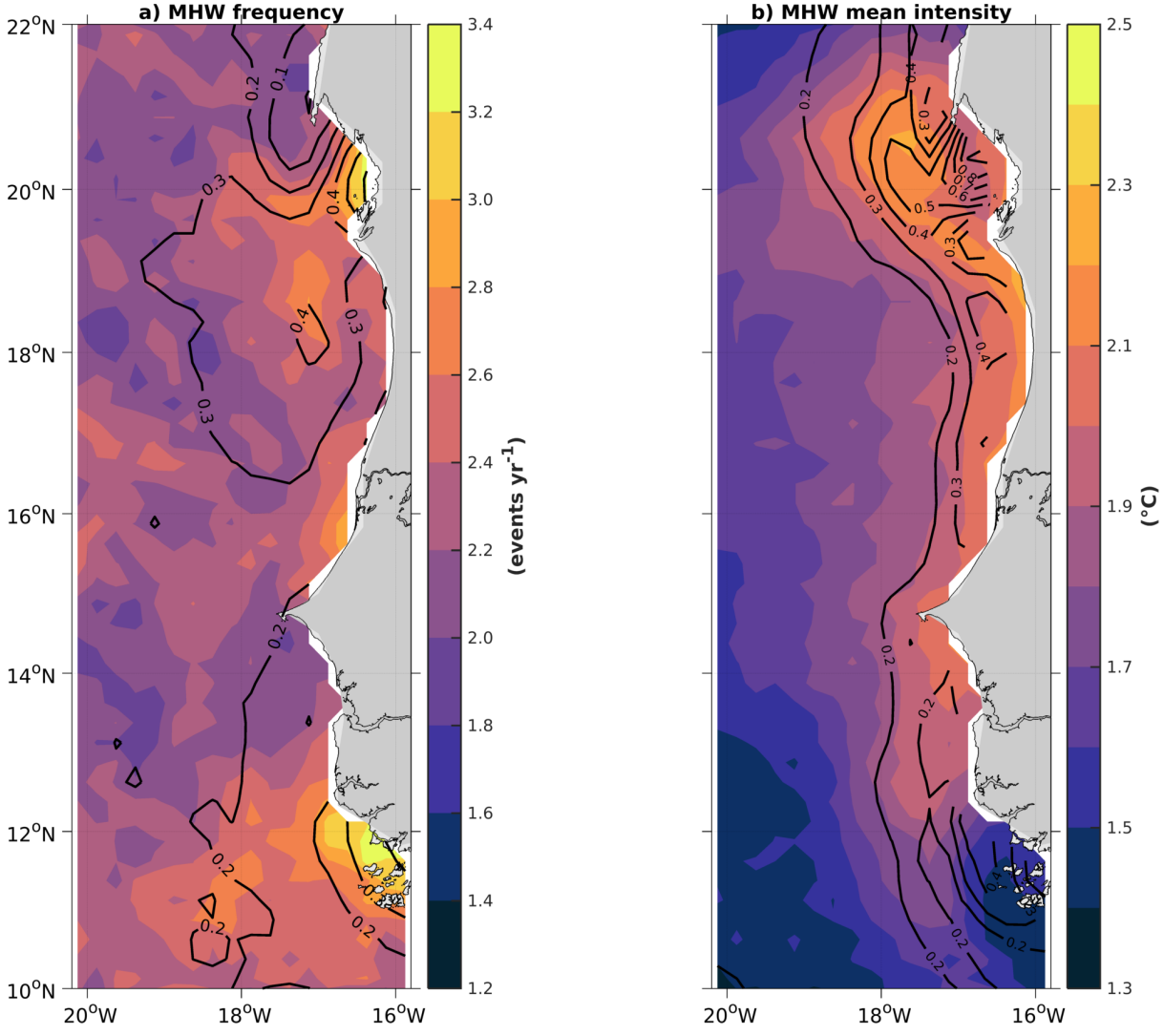

Figure A6. Spatial distribution of the mean annual characteristics of marine heatwaves (MHWs) in the SMUS over the 1982–2024 period: (a) occurrence (events·yr^{-1}) and (b) mean intensity (°C). Black contours in panel (a) represent linear trends in sea surface temperature (SST; °C·decade^{-1}), while those in panel (b) depict the magnitude of the SST spatial gradient.